

preparation, hybridization process and microarray data analysis were performed by TAKARA BIO (Otsu, Japan). The quality of total RNA was assessed with the Agilent 2100 Bioanalyzer, and the RNA integrity number values showed sufficiently high quality (ranging from 8.7 to 9.2). Agilent one-color microarray-based gene expression profiling was used to detect differential gene expression in the spinal cords and skeletal muscles of untreated and PG-treated AR-97Q mice. Array image analysis and the calculation of spot intensity measurements were performed with Agilent's Feature Extraction Software. The criteria used to detect the differences in gene expression were a 2-fold and 3-fold change in the spinal cords and muscles, respectively, of PG-treated AR-97Q mice compared with untreated AR-97Q mice. The expression profiles were analyzed using GeneSpring 12.5 software (Silicon Genetics, CA, USA). The microarray profiling data were deposited in the Gene Expression Omnibus data base with the accession number GSE51807.

Urinary analyses of the AR-97Q mice

The mice were placed in metabolic cages, and urine was collected over a 24-h period. The concentration of 8-OHdG was measured with an ELISA kit for 8-hydroxy-2'-deoxyguanosine (Japan Institute for the Control of Aging (JaICA), Shizuoka, Japan) and that of creatinine was measured with an ELISA kit for creatinine (Cayman) according to the manufacturer's instructions. The urinary levels of 8-OHdG were normalized in relation to creatinine levels to adjust for the urine volume.

Statistical analysis

We analyzed the data using the unpaired Student's *t*-test for two group comparisons and analysis of variance (ANOVA) with Dunnett's test for multiple comparisons using PASW Statistics 18 (Chicago, IL, USA). The survival rate was analyzed by Kaplan–Meier and log-rank tests using STATVIEW software version 5 (Hulinks, Tokyo, Japan). We denoted *P*-values of 0.05 or less as statistically significant.

Study approval

The collection of autopsied human tissues and their use for this study were approved by the Ethics Committee of Nagoya University Graduate School of Medicine (No. 902-3), and written informed consent was obtained from the patients' next-of-kin. Experimental procedures involving human subjects were conducted in conformance with the principles expressed in the Declaration of Helsinki. All of the animal experiments were performed in accordance with the National Institutes of Health Guide for the Care and Use of Laboratory Animals and under the approval of the Nagoya University Animal Experiment Committee (No. 25087).

SUPPLEMENTARY MATERIAL

Supplementary Material is available at *HMG* online.

ACKNOWLEDGEMENT

Pioglitazone was provided by Takeda Pharmaceutical Co., Ltd.

Conflict of Interest statement. None declared.

FUNDING

This work was supported by the Global COE Program, MEXT, Japan; MEXT/JSPS KAKENHI (grant numbers 21229011, 21689024, 22110005, 23390230, 24659428 and 26293206); Health Labor Sciences Research Grants, MHLW, Japan; CREST, JST; a grant from the Kennedy Disease Association and a grant from the Daiichi Sankyo Foundation of Life Science. The investigators had sole discretion over study design, collection, analysis, and interpretation of data, writing of the report, and decision to submit it for publication.

REFERENCES

1. La Spada, A.R. and Taylor, J.P. (2010) Repeat expansion disease: progress and puzzles in disease pathogenesis. *Nat. Rev. Genet.*, **11**, 247–258.
2. Kennedy, W.R., Alter, M. and Sung, J.H. (1968) Progressive proximal spinal and bulbar muscular atrophy of late onset. A sex-linked recessive trait. *Neurology*, **18**, 671–680.
3. Sobue, G., Hashizume, Y., Mukai, E., Hirayama, M., Mitsuma, T. and Takahashi, A. (1989) X-linked recessive bulbospinal neuronopathy. A clinicopathological study. *Brain*, **112**, 209–232.
4. Katsuno, M., Tanaka, F., Adachi, H., Banno, H., Suzuki, K., Watanabe, H. and Sobue, G. (2012) Pathogenesis and therapy of spinal and bulbar muscular atrophy (SBMA). *Prog. Neurobiol.*, **99**, 246–256.
5. Katsuno, M., Adachi, H., Kume, A., Li, M., Nakagomi, Y., Niwa, H., Sang, C., Kobayashi, Y., Doyu, M. and Sobue, G. (2002) Testosterone reduction prevents phenotypic expression in a transgenic mouse model of spinal and bulbar muscular atrophy. *Neuron*, **35**, 843–854.
6. Minamiyama, M., Katsuno, M., Adachi, H., Doi, H., Kondo, N., Iida, M., Ishigaki, S., Fujioka, Y., Matsumoto, S., Miyazaki, Y. *et al.* (2012) Naratriptan mitigates CGRP1-associated motor neuron degeneration caused by an expanded polyglutamine repeat tract. *Nat. Med.*, **18**, 1531–1538.
7. Nedelsky, N.B., Pennuto, M., Smith, R.B., Palazzolo, I., Moore, J., Nie, Z., Neale, G. and Taylor, J.P. (2010) Native functions of the androgen receptor are essential to pathogenesis in a Drosophila model of spinobulbar muscular atrophy. *Neuron*, **67**, 936–952.
8. Katsuno, M., Adachi, H., Minamiyama, M., Waza, M., Tokui, K., Banno, H., Suzuki, K., Onoda, Y., Tanaka, F., Doyu, M. *et al.* (2006) Reversible disruption of dynactin 1-mediated retrograde axonal transport in polyglutamine-induced motor neuron degeneration. *J. Neurosci.*, **26**, 12106–12117.
9. Sorarù, G., D'Ascenzo, C., Polo, A., Palmieri, A., Baggio, L., Vergani, L., Gellera, C., Moretto, G., Pegoraro, E. and Angelini, C. (2008) Spinal and bulbar muscular atrophy: skeletal muscle pathology in male patients and heterozygous females. *J. Neurol. Sci.*, **264**, 100–105.
10. Rhodes, L.E., Freeman, B.K., Auh, S., Kokkinis, A.D., La, P.A., Chen, C., Lehky, T.J., Shrader, J.A., Levy, E.W., Harris, L.M. *et al.* (2009) Clinical features of spinal and bulbar muscular atrophy. *Brain*, **132**, 3242–3251.
11. Hashizume, A., Katsuno, M., Banno, H., Suzuki, K., Suga, N., Mano, T., Atsuta, N., Oe, H., Watanabe, H., Tanaka, F. *et al.* (2012) Longitudinal changes of outcome measures in spinal and bulbar muscular atrophy. *Brain*, **135**, 2838–2848.
12. Chevalier-Larsen, E.S., O'Brien, C.J., Wang, H., Jenkins, S.C., Holder, L., Lieberman, A.P. and Merry, D.E. (2004) Castration restores function and neurofilament alterations of aged symptomatic males in a transgenic mouse model of spinal and bulbar muscular atrophy. *J. Neurosci.*, **24**, 4778–4786.
13. Palazzolo, I., Stack, C., Kong, L., Musaro, A., Adachi, H., Katsuno, M., Sobue, G., Taylor, J.P., Sumner, C.J., Fischbeck, K.H. *et al.* (2009) Overexpression of IGF-1 in muscle attenuates disease in a mouse model of spinal and bulbar muscular atrophy. *Neuron*, **63**, 316–328.
14. Yu, Z., Dadgar, N., Albertelli, M., Gruis, K., Jordan, C., Robins, D.M. and Lieberman, A.P. (2006) Androgen-dependent pathology demonstrates

- myopathic contribution to the Kennedy disease phenotype in a mouse knock-in model. *J. Clin. Invest.*, **116**, 2663–2672.
15. Lieberman, A.P., Zhang, Z., Wang, J., Zhang, C., Li, H. and Xu, Y. (2014) Peripheral androgen receptor gene suppression rescues disease in mouse models of spinal and bulbar muscular atrophy. *Cell Rep.*, **7**, 774–784.
 16. Cortes, C.J., Ling, S.C., Guo, L.T., Hung, G., Tsunemi, T., Ly, L., Tokunaga, S., Lopez, E., Sopher, B.L., Bennett, C.F. *et al.* (2014) Muscle expression of mutant androgen receptor accounts for systemic and motor neuron disease phenotypes in spinal and bulbar muscular atrophy. *Neuron*, **82**, 295–307.
 17. Ranganathan, S., Harmison, G.G., Meyertholen, K., Pennuto, M., Burnett, B.G. and Fischbeck, K.H. (2009) Mitochondrial abnormalities in spinal and bulbar muscular atrophy. *Hum. Mol. Genet.*, **18**, 27–42.
 18. Beauchemin, A.M., Gottlieb, B., Beitel, L.K., Elhaji, Y.A., Pinsky, L. and Trifiro, M.A. (2001) Cytochrome c oxidase subunit Vb interacts with human androgen receptor: a potential mechanism for neurotoxicity in spinobulbar muscular atrophy. *Brain Res. Bull.*, **56**, 285–297.
 19. Cui, L., Jeong, H., Borovecki, F., Parkhurst, C.N., Tanese, N. and Krainc, D. (2006) Transcriptional repression of PGC-1 α by mutant huntingtin leads to mitochondrial dysfunction and neurodegeneration. *Cell*, **127**, 59–69.
 20. Tontonoz, P. and Spiegelman, B.M. (2008) Fat and beyond: the diverse biology of PPAR γ . *Annu. Rev. Biochem.*, **77**, 289–312.
 21. Storer, P.D., Xu, J., Chavis, J. and Drew, P.D. (2005) Peroxisome proliferator-activated receptor- γ agonists inhibit the activation of microglia and astrocytes: implications for multiple sclerosis. *J. Neuroimmunol.*, **161**, 113–122.
 22. Gray, E., Ginty, M., Kemp, K., Scolding, N. and Wilkins, A. (2012) The PPAR- γ agonist pioglitazone protects cortical neurons from inflammatory mediators via improvement in peroxisomal function. *J. Neuroinflammation*, **9**, 63.
 23. Xu, F., Li, J., Ni, W., Shen, Y.W. and Zhang, X.P. (2013) Peroxisome proliferator-activated receptor- γ agonist 15d-prostaglandin J2 mediates neuronal autophagy after cerebral ischemia-reperfusion injury. *PLoS One*, **8**, e55080.
 24. Quintanilla, R.A., Jin, Y.N., Fuenzalida, K., Bronfman, M. and Johnson, G.V. (2008) Rosiglitazone treatment prevents mitochondrial dysfunction in mutant huntingtin-expressing cells: possible role of peroxisome proliferator-activated receptor- γ (PPAR γ) in the pathogenesis of Huntington disease. *J. Biol. Chem.*, **283**, 25628–25637.
 25. Mano, T., Katsuno, M., Banno, H., Suzuki, K., Suga, N., Hashizume, A., Tanaka, F. and Sobue, G. (2012) Cross-sectional and longitudinal analysis of an oxidative stress biomarker for spinal and bulbar muscular atrophy. *Muscle Nerve*, **46**, 692–697.
 26. Zhang, H.L., Xu, M., Wei, C., Qin, A.P., Liu, C.F., Hong, L.Z., Zhao, X.Y., Liu, J. and Qin, Z.H. (2011) Neuroprotective effects of pioglitazone in a rat model of permanent focal cerebral ischemia are associated with peroxisome proliferator-activated receptor γ -mediated suppression of nuclear factor- κ B signaling pathway. *Neuroscience*, **176**, 381–395.
 27. Dehmer, T., Heneka, M.T., Sastre, M., Dichgans, J. and Schulz, J.B. (2004) Protection by pioglitazone in the MPTP model of Parkinson's disease correlates with I κ B α induction and block of NF κ B and iNOS activation. *J. Neurochem.*, **88**, 494–501.
 28. Mandrekar-Colucci, S., Karlo, J.C. and Landreth, G.E. (2012) Mechanisms underlying the rapid peroxisome proliferator-activated receptor- γ -mediated amyloid clearance and reversal of cognitive deficits in a murine model of Alzheimer's disease. *J. Neurosci.*, **32**, 10117–10128.
 29. Chawla, A. (2010) Control of macrophage activation and function by PPARs. *Circ. Res.*, **106**, 1559–1569.
 30. Trushina, E. and McMurray, C.T. (2007) Oxidative stress and mitochondrial dysfunction in neurodegenerative diseases. *Neuroscience*, **145**, 1233–1248.
 31. Seong, I.S., Ivanova, E., Lee, J.M., Choo, Y.S., Fossale, E., Anderson, M., Gusella, J.F., Laramie, J.M., Myers, R.H., Lesort, M. *et al.* (2005) HD CAG repeat implicates a dominant property of huntingtin in mitochondrial energy metabolism. *Hum. Mol. Genet.*, **14**, 2871–2880.
 32. Hervias, I., Beal, M.F. and Manfredi, G. (2006) Mitochondrial dysfunction and amyotrophic lateral sclerosis. *Muscle Nerve*, **33**, 598–608.
 33. Browne, S.E. and Beal, M.F. (2006) Oxidative damage in Huntington's disease pathogenesis. *Antioxid. Redox Signal.*, **8**, 2061–2073.
 34. Panov, A.V., Gutekunst, C.A., Leavitt, B.R., Hayden, M.R., Burke, J.R., Strittmatter, W.J. and Greenamyre, J.T. (2002) Early mitochondrial calcium defects in Huntington's disease are a direct effect of polyglutamines. *Nat. Neurosci.*, **5**, 731–736.
 35. Di Prospero, N.A. and Fischbeck, K.H. (2005) Therapeutics development for triplet repeat expansion diseases. *Nat. Rev. Genet.*, **6**, 756–765.
 36. Thau, N., Knippenberg, S., Körner, S., Rath, K.J., Dengler, R. and Petri, S. (2012) Decreased mRNA expression of PGC-1 α and PGC-1 α -regulated factors in the SOD1G93A ALS mouse model and in human sporadic ALS. *J. Neuropathol. Exp. Neurol.*, **71**, 1064–1074.
 37. Eschbach, J., Schwalenstöcker, B., Soyol, S.M., Bayer, H., Wiesner, D., Akimoto, C., Nilsson, A.C., Birve, A., Meyer, T., Dupuis, L. *et al.* (2013) PGC-1 α is a male-specific disease modifier of human and experimental amyotrophic lateral sclerosis. *Hum. Mol. Genet.*, **22**, 3477–3484.
 38. Kiaei, M., Kipiani, K., Chen, J., Calingasan, N.Y. and Beal, M.F. (2005) Peroxisome proliferator-activated receptor- γ agonist extends survival in transgenic mouse model of amyotrophic lateral sclerosis. *Exp. Neurol.*, **191**, 331–336.
 39. Kiaei, M. (2008) Peroxisome proliferator-activated receptor- γ in amyotrophic lateral sclerosis and huntington's disease. *PPAR Res.*, **2008**, 418765.
 40. Kalonia, H., Kumar, P. and Kumar, A. (2010) Pioglitazone ameliorates behavioral, biochemical and cellular alterations in quinolinic acid induced neurotoxicity: possible role of peroxisome proliferator activated receptor- γ (PPAR γ) in Huntington's disease. *Pharmacol. Biochem. Behav.*, **96**, 115–124.
 41. Park, S.W., Yi, J.H., Miranpuri, G., Satriotomo, I., Bowen, K., Resnick, D.K. and Vemuganti, R. (2007) Thiazolidinedione class of peroxisome proliferator-activated receptor γ agonists prevents neuronal damage, motor dysfunction, myelin loss, neuropathic pain, and inflammation after spinal cord injury in adult rats. *J. Pharmacol. Exp. Ther.*, **320**, 1002–1012.
 42. Landreth, G.E. and Heneka, M.T. (2001) Anti-inflammatory actions of peroxisome proliferator-activated receptor γ agonists in Alzheimer's disease. *Neurobiol. Aging*, **22**, 937–944.
 43. Wayman, N.S., Hattori, Y., McDonald, M.C., Mota-Filipe, H., Cuzzocrea, S., Pisano, B., Chatterjee, P.K. and Thiemermann, C. (2002) Ligands of the peroxisome proliferator-activated receptors (PPAR- γ and PPAR- α) reduce myocardial infarct size. *FASEB J.*, **16**, 1027–1040.
 44. Liu, H.R., Tao, L., Gao, E., Lopez, B.L., Christopher, T.A., Willette, R.N., Ohlstein, E.H., Yue, T.L. and Ma, X.L. (2004) Anti-apoptotic effects of rosiglitazone in hypercholesterolemic rabbits subjected to myocardial ischemia and reperfusion. *Cardiovasc. Res.*, **62**, 135–144.
 45. Bright, J.J., Kanakasabai, S., Chearvae, W. and Chakraborty, S. (2008) PPAR regulation of inflammatory signaling in CNS diseases. *PPAR Res.*, **2008**, 658520.
 46. Dupuis, L., Dengler, R., Heneka, M.T., Meyer, T., Zierz, S., Kassubek, J., Fischer, W., Steiner, F., Lindauer, E., Otto, M. *et al.* (2012) A randomized, double blind, placebo-controlled trial of pioglitazone in combination with riluzole in amyotrophic lateral sclerosis. *PLoS One*, **7**, e37885.
 47. Hunt, M.J. and Morton, A.J. (2005) Atypical diabetes associated with inclusion formation in the R6/2 mouse model of Huntington's disease is not improved by treatment with hypoglycaemic agents. *Exp. Brain Res.*, **166**, 220–229.
 48. Di Filippo, M., Chiasserini, D., Tozzi, A., Picconi, B. and Calabresi, P. (2010) Mitochondria and the link between neuroinflammation and neurodegeneration. *J. Alzheimers Dis.*, **20**, S369–S379.
 49. Stommel, E.W., Van Hoff, R.M., Graber, D.J., Bercury, K.K., Langford, G.M. and Harris, B.T. (2007) Tumor necrosis factor- α induces changes in mitochondrial cellular distribution in motor neurons. *Neuroscience*, **146**, 1013–1019.
 50. Mauro, C., Leow, S.C., Anso, E., Rocha, S., Thotakura, A.K., Tornatore, L., Moretti, M., De Smaele, E., Beg, A.A., Tergaonkar, V. *et al.* (2011) NF- κ B controls energy homeostasis and metabolic adaptation by upregulating mitochondrial respiration. *Nat. Cell. Biol.*, **13**, 1272–1279.
 51. Mariappan, N., Elks, C.M., Sriramula, S., Guggilam, A., Liu, Z., Borkhsenius, O. and Francis, J. (2010) NF- κ B-induced oxidative stress contributes to mitochondrial and cardiac dysfunction in type II diabetes. *Cardiovasc. Res.*, **85**, 473–483.
 52. Kaltschmidt, B. and Kaltschmidt, C. (2009) NF- κ B in the nervous system. *Cold Spring Harb. Perspect. Biol.*, **1**, a001271.
 53. Swarup, V., Phaneuf, D., Dupré, N., Petri, S., Strong, M., Kriz, J. and Julien, J.P. (2011) Deregulation of TDP-43 in amyotrophic lateral sclerosis triggers nuclear factor κ B-mediated pathogenic pathways. *J. Exp. Med.*, **208**, 2429–2447.
 54. Yates, L.L. and Górecki, D.C. (2006) The nuclear factor- κ B (NF- κ B): from a versatile transcription factor to a ubiquitous therapeutic target. *Acta Biochim. Pol.*, **53**, 651–662.

55. Sambataro, F. and Pennuto, M. (2012) Cell-autonomous and non-cell-autonomous toxicity in polyglutamine diseases. *Prog. Neurobiol.*, **97**, 152–172.
56. Ilieva, H., Polymenidou, M. and Cleveland, D.W. (2009) Non-cell autonomous toxicity in neurodegenerative disorders: ALS and beyond. *Cell Biol.*, **187**, 761–772.
57. Boillée, S., Yamanaka, K., Lobsiger, C.S., Copeland, N.G., Jenkins, N.A., Kassiotis, G., Kollias, G. and Cleveland, D.W. (2006) Onset and progression in inherited ALS determined by motor neurons and microglia. *Science*, **312**, 1389–1392.
58. Beers, D.R., Henkel, J.S., Zhao, W., Wang, J. and Appel, S.H. (2008) CD4+ T cells support glial neuroprotection, slow disease progression, and modify glial morphology in an animal model of inherited ALS. *Proc. Natl. Acad. Sci. USA*, **105**, 15558–15563.
59. Henkel, J.S., Beers, D.R., Siklós, L. and Appel, S.H. (2006) The chemokine MCP-1 and the dendritic and myeloid cells it attracts are increased in the mSOD1 mouse model of ALS. *Mol. Cell. Neurosci.*, **31**, 427–437.
60. Kishida, K., Shimomura, I., Nishizawa, H., Maeda, N., Kuriyama, H., Kondo, H., Matsuda, M., Nagaretani, H., Ouchi, N., Hotta, K. *et al.* (2001) Enhancement of the aquaporin adipose gene expression by a peroxisome proliferator-activated receptor gamma. *J. Biol. Chem.*, **276**, 48572–48579.
61. Waza, M., Adachi, H., Katsuno, M., Minamiyama, M., Sang, C., Tanaka, F., Inukai, A., Doyu, M. and Sobue, G. (2005) 17-AAG, an Hsp90 inhibitor, ameliorates polyglutamine-mediated motor neuron degeneration. *Nat. Med.*, **11**, 1088–1095.
62. Katsuno, M., Adachi, H., Minamiyama, M., Waza, M., Doi, H., Kondo, N., Mizoguchi, H., Nitta, A., Yamada, K., Banno, H. *et al.* (2010) Disrupted transforming growth factor-beta signaling in spinal and bulbar muscular atrophy. *J. Neurosci.*, **30**, 5702–5712.
63. Kobayashi, Y., Kume, A., Li, M., Doyu, M., Hata, M., Ohtsuka, K. and Sobue, G. (2000) Chaperones Hsp70 and Hsp40 suppress aggregate formation and apoptosis in cultured neuronal cells expressing truncated androgen receptor protein with expanded polyglutamine tract. *J. Biol. Chem.*, **275**, 8772–8778.
64. Adachi, H., Waza, M., Tokui, K., Katsuno, M., Minamiyama, M., Tanaka, F., Doyu, M. and Sobue, G. (2007) CHIP overexpression reduces mutant androgen receptor protein and ameliorates phenotypes of the spinal and bulbar muscular atrophy transgenic mouse model. *J. Neurosci.*, **27**, 5115–5126.
65. Kondo, N., Katsuno, M., Adachi, H., Minamiyama, M., Doi, H., Matsumoto, S., Miyazaki, Y., Iida, M., Tohnai, G., Nakatsuji, H. *et al.* (2013) Heat shock factor-1 influences pathological lesion distribution of polyglutamine-induced neurodegeneration. *Nat. Commun.*, **4**, 1405.
66. Toyokuni, S., Tanaka, T., Hattori, Y., Nishiyama, Y., Yoshida, A., Uchida, K., Hiai, H., Ochi, H. and Osawa, T. (1997) Quantitative immunohistochemical determination of 8-hydroxy-2'-deoxyguanosine by a monoclonal antibody N45.1: its application to ferric nitrilotriacetate-induced renal carcinogenesis model. *Lab. Invest.*, **76**, 365–374.

Brugada syndrome in spinal and bulbar muscular atrophy



Amane Araki, MD
Masahisa Katsuno, MD
Keisuke Suzuki, MD
Haruhiko Banno, MD
Noriaki Suga, MD
Atsushi Hashizume, MD
Tomoo Mano, MD
Yasuhiro Hijikata, MD
Hideaki Nakatsuji, MD
Hirohisa Watanabe, MD
Masahiko Yamamoto, MD
Takeru Makiyama, MD
Seiko Ohno, MD
Megumi Fukuyama, MD
Shin-ichiro Morimoto, MD
Minoru Horie, MD
Gen Sobue, MD

Correspondence to
Dr. Katsuno:
ka2no@med.nagoya-u.ac.jp
or Dr. Sobue:
sobueg@med.nagoya-u.ac.jp

ABSTRACT

Objective: The aim of this study was to clarify myocardial involvement and its clinical implications in subjects with spinal and bulbar muscular atrophy (SBMA), a neuromuscular disease affecting both neuronal and nonneuronal tissues.

Methods: Two independent cardiologists evaluated ECGs from a total of 144 consecutive subjects with SBMA. We performed immunohistochemical, immunoblot, and quantitative real-time PCR analyses of autopsied myocardium.

Results: Abnormal ECGs were detected in 70 (48.6%) of 144 subjects. The most frequent findings were ST-segment abnormalities in V_{1-3} (19.4%), followed by ST-segment abnormalities in V_{5-6} (18.1%). We detected Brugada-type ECGs in 17 of 28 subjects with ST-segment abnormalities in V_{1-3} . Of those, one subject presented with syncope that required an implantable cardioverter defibrillator and led to eventual sudden death, and another subject also died suddenly. No subjects with Brugada-type ECGs had mutations in *SCN5A*, *CACNA1C*, or *CACNB2* genes. In autopsied cases, we detected nuclear accumulation of the mutant androgen receptor protein and decreased expression levels of *SCN5A* in the myocardium.

Conclusions: Subjects with SBMA often show Brugada-type ECG. The accumulation of the pathogenic androgen receptor may have a role in the myocardial involvement in SBMA. *Neurology*® 2014;82:1813-1821

GLOSSARY

AR = androgen receptor; **CACNA1C** = calcium channel, voltage-dependent, L type, α 1C subunit; **CACNB2** = calcium channel, voltage-dependent, β 2 subunit; **GAPDH** = glyceraldehyde-3-phosphate dehydrogenase; **HEY2** = hes-related family bHLH transcription factor with YRPW motif 2; **SBMA** = spinal and bulbar muscular atrophy; **SCN5A** = sodium channel, voltage-gated, type V, α subunit; **SCN10A** = sodium channel, voltage-gated, type X, α subunit.

Spinal and bulbar muscular atrophy (SBMA), or Kennedy disease, is a hereditary neuromuscular disease caused by the expansion of a trinucleotide CAG repeat in the androgen receptor (*AR*) gene.^{1,2} SBMA occurs predominately in adult males.^{3,4} The accumulation of the pathogenic AR proteins in the nucleus of motor neurons is central to the pathogenesis of this disease.⁵

In addition to neuromuscular deficits, nonneuronal symptoms such as gynecomastia, muscle cramps, hypertension, hyperlipidemia, and liver dysfunction are often observed in patients with SBMA.^{4,6} While gynecomastia and other symptoms of androgen insensitivity appear to result from the partial loss of AR function, the remaining nonneuronal symptoms are likely due to toxicity of the pathogenic AR in these tissues.^{7,8} In particular, the elevated serum levels of creatine kinase together with histopathologic findings of myopathic changes indicate the role of skeletal muscle damage in the pathogenesis of SBMA.⁹⁻¹¹

Although the nuclear accumulation of the pathogenic AR protein is observed in autopsied myocardium,⁷ clinical signs of cardiac disease have not been fully evaluated.¹² In an effort to elucidate the myocardial pathology and its clinical implication in SBMA, we analyzed electrophysiologic, histopathologic, and biochemical properties of the myocardium of SBMA, and

Supplemental data
at Neurology.org

From the Department of Neurology (A.A., M.K., K.S., H.B., N.S., A.H., T. Mano, Y.H., H.N., H.W., G.S.), Nagoya University Graduate School of Medicine; Institute for Advanced Research (H.B.), Nagoya University; Department of Speech Pathology and Audiology (M.Y.), Aichi-Gakuin University School of Health Science, Nishin; Department of Cardiovascular Medicine (T. Makiyama), Kyoto University Graduate School of Medicine; Department of Cardiovascular and Respiratory Medicine (S.O., M.F., M.H.), Shiga University of Medical Science, Ohtsu; and Division of Cardiology (S.-i.M.), Department of Internal Medicine, Fujita Health University School of Medicine, Toyoake, Japan.

Go to Neurology.org for full disclosures. Funding information and disclosures deemed relevant by the authors, if any, are provided at the end of the article.

found that subjects with SBMA may show Brugada-type ECG, which is an ECG representation of a coved or saddle-back-type ST-segment elevation in ≥ 1 lead among the right precordial leads V_{1-3} , and is associated with sudden death.^{13,14}

METHODS Patients. Subjects were 144 consecutive Japanese subjects with SBMA (aged 52.1 ± 10.1 years). We included genetically confirmed male Japanese subjects with more than one of the following symptoms: muscle weakness, muscle atrophy, or bulbar palsy. The subjects were excluded if they met any of the following criteria: (1) severe complications such as malignancy; (2) other neurologic complications; (3) had taken hormonal agents within 48 weeks before informed consent; or (4) participated in any other clinical trials before informed consent. All subjects were outpatients and were followed in Nagoya University Hospital. The data were collected between February 2002 and August 2012.

Evaluation of ECG. Standard 12-lead ECG was recorded from all of the participants and evaluated by 2 independent cardiologists. The diagnosis of the Brugada-type ECG or Brugada syndrome was made on the basis of the second consensus conference.¹⁴ In the subjects with Brugada-type abnormality on standard 12-lead ECG, we also examined ECG in which the right precordial leads were placed to the third intercostal spaces for classifying 3 types of Brugada-type ECGs. We did not perform the sodium channel blocker challenge test in subjects with type 2 or 3 Brugada-type ECG.

Evaluation of disease severity and serologic parameters. We evaluated disease severity using the revised Amyotrophic Lateral Sclerosis Functional Rating Scale, a validated questionnaire-based scale that measures physical function performing activity of daily living as described previously.¹⁵ We defined the onset of disease as the time when muscle weakness began, but not when tremor of the fingers appeared. Serum levels of testosterone were measured by radioimmunoassay in the subjects who were evaluated until 2006 and by chemiluminescent immune assay in the others.

Histopathology. We analyzed autopsied myocardial specimens of 7 genetically diagnosed subjects with SBMA and 4 sex- and age-matched control subjects (aged 66.7 ± 9.7 and 69.5 ± 5.8 years at the time of death, respectively) using immunohistochemistry. Pathologic diagnoses of the controls were malignant lymphoma, dementia with Lewy bodies, corticobasal degeneration, and progressive supranuclear palsy. The myocardia were excised at autopsy and fixed immediately in 10% buffered formalin solution. Sections (6 μm) were deparaffinized, treated with microwave heating for 10 minutes in 10 mM citrate buffer at pH 6.0, and incubated with primary antibodies. Subsequent staining procedures were performed using the Envision+ kit (Dako, Glostrup, Denmark) as described previously.¹⁶ For anti-polyglutamine staining, sections were treated with 98% formic acid at room temperature for 3 minutes before the antigen retrieval with the microwave. We used the following primary antibodies: AR (N-20, 1:1,000; Santa Cruz Biotechnology, Dallas, TX); SCN5A (sc-22758, 1:1,000; Santa Cruz); and polyglutamine 1C2 (MAB1574, 1:20,000; Millipore Corp., Billerica, MA).

Immunoblotting. We analyzed autopsied myocardial specimens of 4 genetically diagnosed subjects with SBMA and 4 sex- and age-matched control subjects (aged 66.8 ± 11.0 and

69.5 ± 5.8 years at the time of death, respectively) using immunoblotting. Autopsied myocardial specimens were homogenized in CellLytic lysis buffer (Sigma-Aldrich, St. Louis, MO) containing a phosphatase inhibitor cocktail (Sigma-Aldrich) and a protease inhibitor cocktail (Thermo Scientific, Waltham, MA). Homogenates were then centrifuged at 2,500g for 10 minutes at 4°C. The supernatant fractions were separated on 5% to 20% SDS-polyacrylamide gel electrophoresis gels and transferred to Hybond-P membranes (GE Healthcare, Buckinghamshire, UK). Primary antibody binding was probed using horseradish peroxidase-conjugated secondary antibodies (GE Healthcare) at a dilution of 1:5,000, and bands were detected using the ECL prime kit (GE Healthcare). The immunoblots were digitalized (LAS-3000 imaging system; Fujifilm), signal intensities were quantified with Image Gauge software version 4.22 (Fujifilm), and the means \pm SEM were expressed in arbitrary units. The following primary antibodies were used: anti-SCN5A (sc-23174, 1:1,000; Santa Cruz) and anti-GAPDH (MAB374, 1:5,000; Millipore).

Quantitative real-time PCR. Quantification of messenger RNA levels was determined by real-time PCR as described previously.¹⁷ Briefly, total RNA was extracted from autopsied myocardium using RNeasy Fibrous Tissue Midi Kit (Qiagen, Venlo, Limburg). The extracted RNA was reverse-transcribed into first-strand complementary DNA using SuperScript III reverse transcriptase (Invitrogen). Detailed methods for real-time PCR are described in appendix e-1 on the *Neurology*[®] Web site at Neurology.org.

Genetic analysis. Genomic DNA was extracted from peripheral blood of subjects with SBMA using conventional techniques. PCR amplification of the CAG repeat in the *AR* gene was performed using a fluorescein-labeled forward primer (5'-TCCAGAATCTGTTCCAGAGCGTGC-3') and a nonlabeled reverse primer (5'-TGGCCTCGCTCAGGATGTCTTTAAG-3'). Detailed PCR conditions were described previously.¹⁸ Aliquots of PCR products were combined with loading dye and separated by electrophoresis with an autoread sequencer (SQ-5500; Hitachi Electronics Engineering, Tokyo, Japan). In subjects with Brugada-type ECGs, we screened for sodium channel, voltage-gated, type V, α subunit (*SCN5A*), calcium channel, voltage-dependent, L type, $\alpha 1C$ subunit (*CACNA1C*), and calcium channel, voltage-dependent, $\beta 2$ subunit (*CACNB2*) mutations, which are representative genes linked to Brugada syndrome, using a high-resolution melting method or denaturing high-performance liquid chromatography (WAVE system model 3500; Transgenomic, Omaha, NE) and subsequent direct sequencing, as previously reported.^{19,20}

Standard protocol approvals, registrations, and patient consents. This study adhered to the Ethics Guidelines for Human Genome/Gene Analysis Research and those for Epidemiological Studies endorsed by the Japanese government, and was approved by the Ethics Committees of Nagoya University Graduate School of Medicine, Kyoto University Graduate School of Medicine, and Shiga University of Medical Science. All participants provided written informed consent. The collection of autopsied human tissues and their use for this study were also approved by the Ethics Committee of Nagoya University Graduate School of Medicine, and written informed consent was obtained from the subjects' next of kin. Experimental procedures involving human subjects were conducted in conformance with the principles expressed in the Declaration of Helsinki.

Table 1 Clinical features and blood chemical values of subjects with SBMA

	Mean ± SD	Range	No.
Age at examination, y	52.1 ± 10.1	27-75	144
Duration from onset, y	8.7 ± 5.1	1-25	144
Age at onset, y	43.5 ± 9.7	22-69	144
CAG repeat size in AR gene	48.1 ± 3.3	40-57	144
ALSFERS-R (normal score = 48)	42.4 ± 3.9	29-48	144
Systolic blood pressure, mm Hg	130.0 ± 18.9	92-190	144
Diastolic blood pressure, mm Hg	81.5 ± 11.8	53-115	144
Hemoglobin A1c (NGSP), %	5.8 ± 0.8	4.6-9.3	144
Total cholesterol, mg/dL	213.9 ± 36.7	140-342	144
Triglyceride, mg/dL	175.2 ± 103.5	49-651	144
Sodium, mEq/L	140.8 ± 1.9	136-146	144
Potassium, mEq/L	4.3 ± 0.4	3.4-5.8	144
Testosterone (RIA), ng/mL	6.5 ± 1.8	2.9-10.2	68
Testosterone (CLIA), ng/mL	7.8 ± 3.0	3.4-15.0	75

Abbreviations: ALSFRS-R = revised Amyotrophic Lateral Sclerosis Functional Rating Scale; AR = androgen receptor; CLIA = chemiluminescent immune assay; NGSP = National Glycohemoglobin Standardization Program; RIA = radioimmunoassay; SBMA = spinal and bulbar muscular atrophy. Serum levels of testosterone were measured by RIA in the subjects evaluated until 2006 and by CLIA in the others.

Statistical analysis. All data are presented as means ± SD. Intergroup differences in categorical and continuous variables were assessed using the χ^2 test and unpaired *t* test, respectively. A *p* value <0.05 was considered to indicate significance. Calculations were performed using the statistical software package SPSS 20.0J (SPSS Japan, Tokyo, Japan).

RESULTS Patient demographics and blood profiles.

The clinical and hematologic features of the 144 subjects with SBMA are described in table 1. The characteristics of the present study population, such as age at examination, age at onset, and CAG repeat length, were similar to those of previous studies.^{21,22} Hypertension, hypercholesterolemia, and hypertriglyceridemia were observed in 37.6%, 41.7%, and 49.3% of the subjects, respectively. Histories of cardiovascular disease included angina in 4 cases, and myocardial infarction, aortic regurgitation, bradycardia, pulmonary artery stenosis with ventricular septal defect, arrhythmia, cardiac hypertrophy, or aortic dissection in one case each.

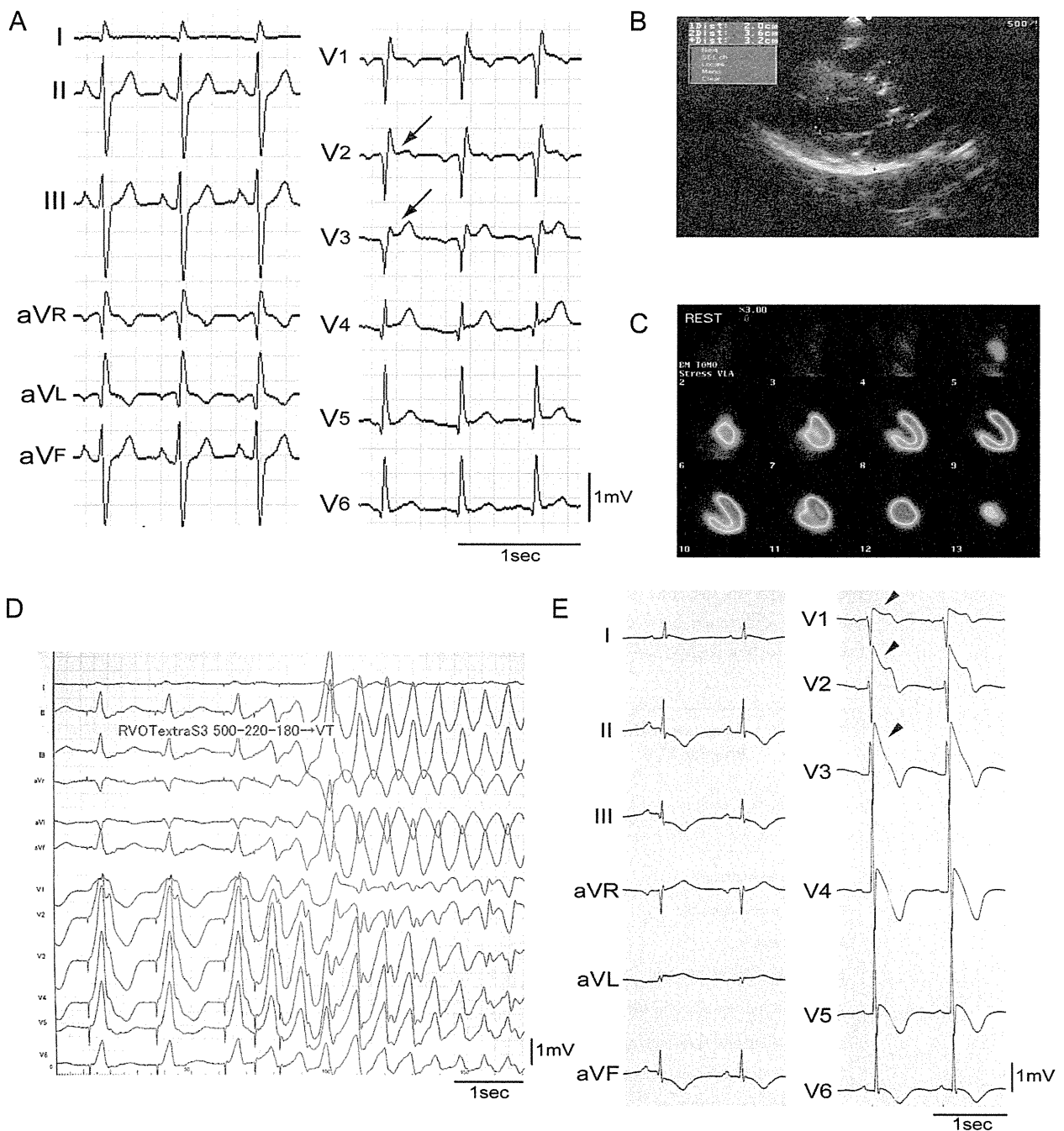
ECG abnormalities. Seventy (48.6%) of 144 subjects showed an abnormal ECG. The most frequent findings were ST-segment abnormalities in V₁₋₃ (19.4%), followed by ST-segment abnormalities in I, aVL, V₅₋₆ (18.1%), left ventricular hypertrophies (9.7%), ST-segment abnormalities in II, aVF (7.6%), and right bundle branch blocks (5.6%). Among the ST-segment abnormalities in right precordial leads (V₁₋₃), the most common feature was Brugada-type ECGs, which were detected in 17 of 144 subjects

(11.8%) in our cohort. The Brugada-type ECGs in subjects with SBMA were classified into 3 subtypes¹³: type 1 in 6 subjects, type 2 in 7 subjects, and type 3 in 4 subjects.

Case reports. Two subjects were diagnosed with symptomatic Brugada syndrome among the 17 cases with Brugada-type ECG. One of these subjects experienced syncope, and both of them had sudden death. The detailed clinical findings of these subjects are described below.

Case 1. Case 1 (patient 1 in table e-1), a 75-year-old man with a history of SBMA, presented with syncope. His medical history included benign prostatic hyperplasia and glaucoma, but he did not have any heart diseases. At the age of 40 years, he experienced the first syncope and medical examination revealed a right bundle branch block. He noticed muscle weakness of his limbs at age 65 years and was diagnosed with SBMA by genetic screening (CAG repeat length was 46). He had his second syncope after drinking at the age of 78 years but regained consciousness 5 minutes later. His ECG showed type 2 Brugada ECG (figure 1A). Neither his echocardiogram nor iodine-123- β -methyl iodophenyl pentadecanoic acid myocardial scintigram demonstrated any detectable left ventricular dysfunction (figure 1, B and C). There were no abnormalities in heart coronary arteries with contrast, but the electrophysiologic study induced ventricular tachycardia by extra-stimuli from the right ventricular outflow tract, in which the basic

Figure 1 Representative cases of SBMA and Brugada pattern ECG



(A-D) Standard ECG (A), echocardiogram (B), ^{123}I -BMIPP myocardial scintigram (C), and ECG in the electrophysiologic study from the RVOT (D) of case 1. The arrows indicate the saddle-back-type ST-segment elevation that is characteristic of type 2 Brugada ECG (A). (E) Standard ECG of case 2 recorded just before death. The arrowheads indicate the coved-type ST-segment elevation, indicating type 1 Brugada ECG. ^{123}I -BMIPP = iodine-123- β -methyl iodophenyl pentadecanoic acid; RVOT = right ventricular outflow tract; SBMA = spinal and bulbar muscular atrophy.

ventricular stimulation period was 500 milliseconds, and 2 consecutive stimulation periods were 220 and 180 milliseconds (figure 1D). He received an implantable cardioverter defibrillator under the diagnosis of Brugada syndrome, but it was removed 2 years later because of a bacterial infection. At age 82 years, he was hospitalized for pneumonia and dehydration, and died suddenly when he was sleeping at night. His last temperature was 37.5°C. His sodium

and potassium levels on the date of death were 164 and 3.6 mEq/L (normal ranges were 138–146 and 3.6–4.9 mEq/L), respectively. No autopsy was performed on this subject.

Case 2. Case 2 (patient 2 in table e-1), a 68-year-old man with a history of SBMA, presented with sudden death. His medical history was unremarkable except for high blood pressure, diabetes mellitus, traumatic subarachnoid hemorrhage, and spasmodic deafness.

He noticed dysphagia and muscle weakness of his limbs at the age of 50 years. He was diagnosed with SBMA by genetic screening (CAG repeat length was 50). At age 70 years, he suddenly lost consciousness at the moment when he moved to a dining table with the assistance of his family at night, following loss of appetite for 1 week. His sodium and potassium levels were 115 and 3.8 mEq/L, respectively. His ECG showed pulseless electrical activity with ST elevations in V₁₋₄ (type 1 Brugada ECG) (figure 1E). Despite cardiopulmonary resuscitations, he died 23 minutes after the onset of unconsciousness. A mild bronchial pneumonia, a mild ischemia-related heart change, and arteriosclerosis of coronary arteries were indicated at autopsy, but histopathologic analysis did not identify the direct cause of death. Acute heart failure due to arrhythmia was suspected as the cause of death.

Clinical features of the subjects with Brugada-type ECGs. Longer CAG repeat sizes and higher serum testosterone levels tended to occur in subjects with Brugada-type ECGs compared with those without Brugada-type ECGs, but there was no statistically significant difference between the groups in clinical features and blood chemical values (table 2). PQ and

QRS intervals were also equivalent between the groups. The details of 17 subjects with SBMA and Brugada-type ECG are shown in table e-1. One of 14 subjects who underwent echocardiography had a right ventricular overload and mild tricuspid regurgitation, whereas no evidence of myocardial dysfunction was found in the remaining 13 subjects. None of the 17 subjects with Brugada-type ECGs had family histories of sudden cardiac deaths at an age younger than 45 years, symptomatic bradycardia, or coved-type ECGs in their family members. Genetic analysis demonstrated no known gene mutations in conjunction with Brugada syndrome in the 17 subjects, including *SCN5A*, *CACNA1C*, and *CACNB2* genes.

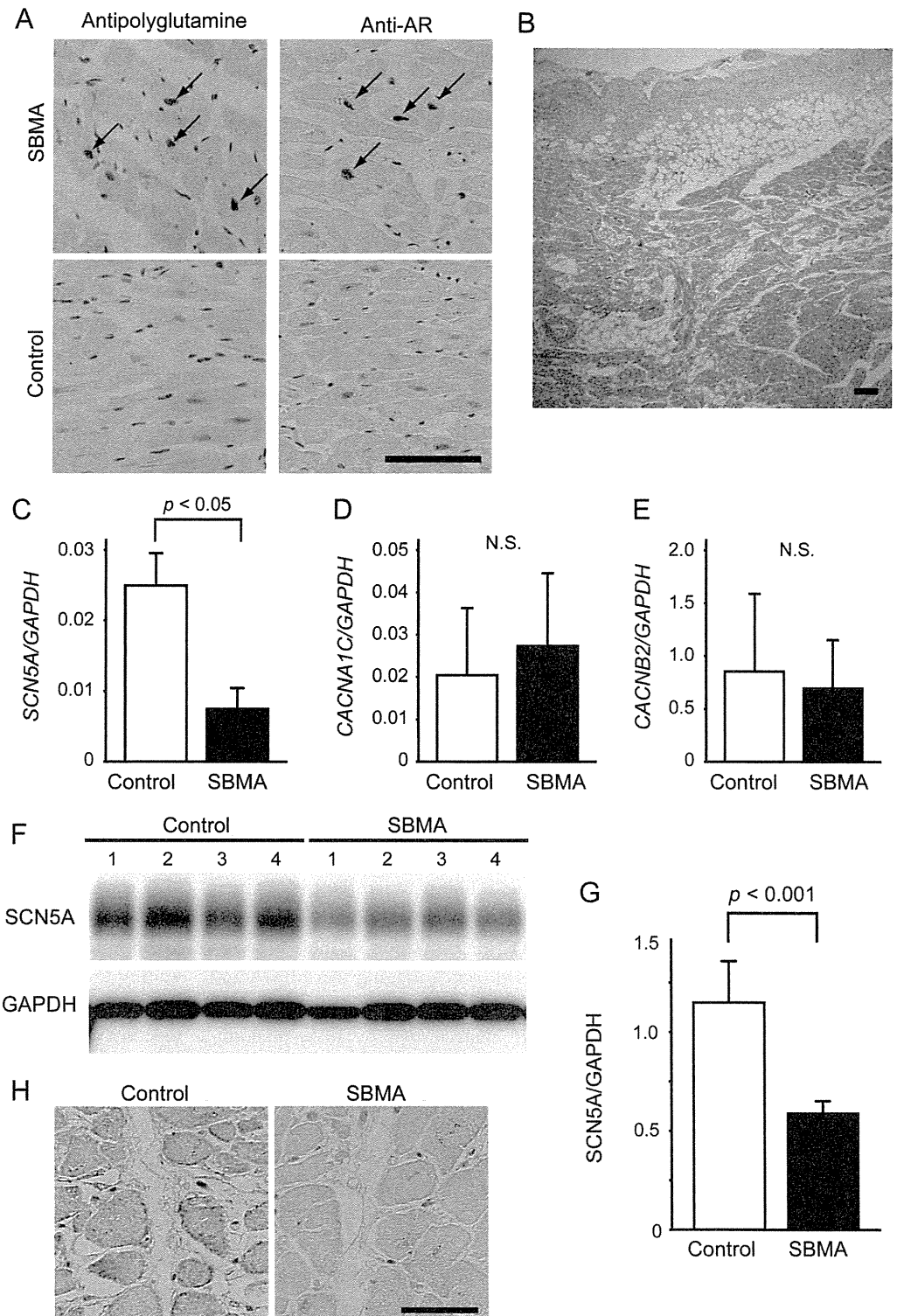
Histopathologic and biochemical study. Histopathologic analyses of the myocardium revealed nuclear accumulation of the pathogenic AR in all 7 autopsied subjects with SBMA (figure 2A), of which one had symptomatic Brugada syndrome as described above (case 2). Hematoxylin & eosin staining showed no detectable abnormalities, except for one subject with increased fat tissue within the right ventricle myocardium, which was reported previously in subjects with Brugada syndrome (figure 2B).²³ To elucidate the molecular basis of Brugada-type ECG in SBMA, we

Table 2 Comparison of clinical, blood chemical, and ECG findings of subjects with SBMA with or without Brugada ECG

	With Brugada-type ECG		Without Brugada-type ECG		p
	Mean ± SD	No.	Mean ± SD	No.	
Age at examination, y	51.5 ± 13.6	17	52.2 ± 9.6	127	NS
Duration from onset, y	8.2 ± 5.2	17	8.7 ± 5.1	127	NS
Age at onset, y	43.4 ± 11.0	17	43.5 ± 9.5	127	NS
CAG repeat size in AR gene	49.5 ± 3.9	17	47.9 ± 3.2	127	NS
ALSFRS-R (normal score = 48)	43.2 ± 2.7	17	42.3 ± 4.0	127	NS
Systolic blood pressure, mm Hg	133.1 ± 28.0	17	129.6 ± 17.5	127	NS
Diastolic blood pressure, mm Hg	83.1 ± 14.9	17	81.3 ± 11.4	127	NS
Hemoglobin A1c (NGSP), %	6.0 ± 1.0	17	5.8 ± 0.8	127	NS
Total cholesterol, mg/dL	204.4 ± 40.8	17	215.1 ± 36.1	127	NS
Triglyceride, mg/dL	146.2 ± 70.8	17	179.1 ± 106.7	127	NS
Sodium, mEq/L	140.7 ± 2.3	17	140.9 ± 1.8	127	NS
Potassium, mEq/L	4.3 ± 0.5	17	4.3 ± 0.3	127	NS
Testosterone (RIA), ng/mL	6.3 ± 2.4	8	6.6 ± 1.8	60	NS
Testosterone (CLIA), ng/mL	9.5 ± 3.2	9	7.6 ± 2.9	66	NS
Heart rate, bpm	77.9 ± 17.6	17	72.4 ± 12.5	127	NS
PQ interval, ms	163 ± 17	17	157 ± 21	127	NS
QRS interval, ms	107 ± 13	17	104 ± 11	127	NS

Abbreviations: ALSFRS-R = revised Amyotrophic Lateral Sclerosis Functional Rating Scale; AR = androgen receptor; bpm = beats per minute; CLIA = chemiluminescent immune assay; NGSP = National Glycohemoglobin Standardization Program; NS = not significant; RIA = radioimmunoassay; SBMA = spinal and bulbar muscular atrophy. Serum levels of testosterone were measured by RIA in the subjects evaluated until 2006 and by CLIA in the others.

Figure 2 Histopathologic and biochemical features of myocardium from subjects with SBMA



(A) Immunohistochemistry using antibodies against AR and expanded polyglutamine and hematoxylin & eosin staining of the myocardium of representative subjects. Arrows indicate the nuclear accumulation of the pathogenic AR in SBMA. (B) Fat deposition in the right ventricle myocardium in one subject with SBMA. (C-E) The messenger RNA levels of CACNA1C (C), CACNB2 (D), and SCN5A (E) measured with quantitative real-time PCR. (F) Immunoblots of SCN5A and GAPDH in myocardium from SBMA and control subjects. (G) Quantification of anti-SCN5A immunoreactive bands. The amount of protein is demonstrated as the ratio for GAPDH. (H) Immunohistochemistry using antibodies against SCN5A in the myocardium from SBMA and control subjects. Scale bars indicate 50 μ m. AR = androgen receptor; CACNA1C = calcium channel, voltage-dependent, L type, α 1C subunit; CACNB2 = calcium channel, voltage-dependent, β 2 subunit; GAPDH = glyceraldehyde-3-phosphate dehydrogenase; SBMA = spinal and bulbar muscular atrophy; SCN5A = sodium channel, voltage-gated, type V, α subunit.

investigated the gene expression of ion channels that are firmly linked to Brugada syndrome. The results of quantitative real-time PCR showed a marked decrease in messenger RNA levels of *SCN5A* but not *CACNA1C* or *CACNB2* in the myocardium of subjects with SBMA (figure 2, C–E). Decreased protein levels of *SCN5A* were also detected by immunoblot (figure 2, F and G) and immunohistochemistry (figure 2H).

DISCUSSION In the present study, we demonstrated that subjects with SBMA exhibit several forms of ECG abnormalities. The most striking observation in our cohort is that Brugada-type ECG was observed in more than 10% of the subjects with SBMA. Of those, 2 subjects reported symptomatic Brugada syndrome, leading to sudden death. Although sudden death by neuronal loss in the intermediolateral nucleus was reported in amyotrophic lateral sclerosis,²⁴ there are no reports of Brugada syndrome, suggesting that this type of ECG appears to be specific to SBMA.

Brugada syndrome may cause sudden death by ventricular fibrillation at an average age of 41 years, without structural heart problems.^{14,25} This syndrome may be responsible for 4% to 12% of all sudden deaths, and at least 20% of sudden deaths in patients with structurally normal hearts. Brugada-type ECG is observed frequently in asymptomatic patients.²⁶ Given that the frequency of Brugada-type ECG is reported to be 0.15% to 1.22% in Japanese community-based populations,^{27,28} our study suggests a very high prevalence of Brugada-type ECGs in SBMA and implies a link between the pathogenesis of the disorders, although we cannot fully exclude the possibility of a chance association of these 2 conditions. In this regard, it is intriguing that SBMA and Brugada syndrome share common clinical features. Both diseases are characterized by male predominance. SBMA affects males exclusively, whereas females with homozygous mutation of the *AR* gene manifest no neuromuscular phenotype.²⁹ Similarly, Brugada syndrome is known to show a high male predominance (80%–90%).¹⁴ The pathologic process of SBMA is dependent on circulating levels of testosterone,^{5,30–32} and high testosterone levels increase the risk of Brugada syndrome via intensifying ionic current imbalance in the myocardium.³³ These commonalities may underlie the high prevalence of Brugada-type ECGs in SBMA. Although another epidemiologic study in 25 European patients with SBMA showed no ECG abnormalities,³⁴ the discrepancy between this and our studies may be attributable to the difference in the sample size and ethnic background. Brugada syndrome is more common in Asian than Caucasian populations,^{14,25,35} which may contribute to the high occurrence of Brugada-type

ECGs in Japanese subjects with SBMA in the present study.

Typical Brugada-type ST elevation (J point elevation) results from an ion current imbalance across cardiac cell membrane, which is induced by the malfunction of cardiac ion channels governing the action potential. Mutations in genes encoding these ion channels or their modulating proteins have been shown to be causative of Brugada syndrome. Among them, mutations in *SCN5A*, which encodes the α subunit of cardiac sodium channel, have been reported in 10% to 30% of patients with Brugada syndrome.¹⁴ Although much less frequent, several other causative genes have also been identified, including the L-type calcium channel (*CACNA1C* and *CACNB2*), glycerol-3-phosphate dehydrogenase 1-like channel, and potassium channels. Recently, a genome-wide association analysis also identified susceptibility loci at *SCN5A*, *SCN10A*, and the *HEY2* genes for Brugada syndrome.³⁶ Although none of our subjects with Brugada-type ECG had mutations in *SCN5A*, *CACNA1C*, or *CACNB2*, histopathologic and biochemical analyses indicated downregulation of *SCN5A* gene expression in the myocardium of subjects with SBMA. Given that the mutations in the *SCN5A* gene are shown to culminate in functional loss of the sodium channels,³⁷ decreased expression of this gene in the myocardium may be associated with the pathogenesis of myocardial involvement in SBMA. Nonneuronal cells, such as hepatocytes and epithelial cells of scrotal skin, show the accumulation of the pathogenic AR, which, at least partially, corresponds to clinical symptoms and findings of SBMA.⁸ Nuclear accumulation of the pathogenic AR induces transcriptional dysregulation, leading to altered expression of several genes in skeletal muscles, as well as the spinal cord.^{38,39} Taken together, gene expression abnormalities due to the nuclear accumulation of pathogenic AR may result in myocardial dysfunction in SBMA.

In the present study, we detected no differences in clinical and genetic features between SBMA subjects with and without Brugada-type ECG, but severe hyponatremia in the subject with symptomatic Brugada syndrome (case 2) suggests that patients with SBMA have the potential risk of Brugada syndrome at basal conditions and that certain triggers (such as hyponatremia) may enhance the electrophysiologic deficits in the myocardium and manifest Brugada-type ECGs or fatal ventricular arrhythmias. This hypothesis is consistent with the observation that Brugada ECG patterns may be modulated by numerous factors, including the autonomic nervous system, altered levels of electrolytes, heavy meals, and high body temperature.²⁶ In particular, hypokalemia in conjunction with hyponatremia is reported to

precipitate Brugada syndrome, as shown in the present study.⁴⁰

Although respiratory tract infections due to bulbar palsy are common at advanced stages of SBMA, the cause of death is not determined in a certain population.²¹ Our results indicate that sudden death due to fatal arrhythmias associated with Brugada syndrome may occur in patients with SBMA. Because subjects with Brugada type 1 ECG are often symptomatic and at a high risk of sudden death, it is important to examine ECGs in patients with SBMA and to carefully manage subjects with Brugada-type ECG abnormalities.

AUTHOR CONTRIBUTIONS

A.A.: drafting the manuscript, analysis/interpretation of the data, acquisition of data, statistical analysis, research project execution, study design and concept. M.K.: revising the manuscript, analysis/interpretation of the data, acquisition of data, statistical analysis, research project execution, study design and concept. K.S., H.B., N.S., A.H., T. Mano, and Y.H.: analysis/interpretation of the data, acquisition of data. H.N.: analysis/interpretation of the data. H.W.: analysis/interpretation of the data, research project execution. M.Y.: analysis/interpretation of the data, acquisition of data. T. Makiyama, S.O., and M.F.: acquisition of data, analysis/interpretation of the data. S.M.: analysis/interpretation of the data, research project execution. M.H.: analysis/interpretation of the data, research project execution, study design and concept. G.S.: research project organization, research project execution, revising the manuscript, interpretation of the data, statistical analysis, study design and concept.

STUDY FUNDING

Supported by a Grant-in-Aid for Scientific Research on Innovated Areas "Foundation of Synapse and Neurocircuit Pathology," and Grants-in-Aid (KAKENHI) from the Ministry of Education, Culture, Sports, Science, and Technology of Japan (22110005, 21229011, and 23390230); grants from the Ministry of Health, Labor and Welfare of Japan; and Core Research for Evolutional Science and Technology (CREST) from the Japan Science and Technology Agency (JST); and a Translational Research grant from the Japanese Circulation Society.

DISCLOSURE

A. Araki reports no disclosures relevant to the manuscript. M. Katsuno is supported by a Grant-in-Aid for Scientific Research on Innovated Areas "Foundation of Synapse and Neurocircuit Pathology" from MEXT, Japan (22110005); KAKENHI grants from MEXT/JSPS, Japan (21229011, 23390230); and CREST from the JST. K. Suzuki, H. Banno, N. Suga, A. Hashizume, T. Mano, Y. Hijikata, H. Nakatsuji, H. Watanabe, M. Yamamoto, T. Makiyama, S. Ohno, M. Fukuyama, and S. Morimoto report no disclosures relevant to the manuscript. M. Horie is supported by a Grant-in-Aid for Scientific Research from the Japan Society for the Promotion of Science (KAKENHI) and a Translational Research grant from the Japanese Circulation Society. G. Sobue serves as a scientific advisory board member for the Kanoe Science Foundation for the Promotion of Medical Science, Naito Science Foundation; an advisory board member of *Brain*; and an editorial board member of *Degenerative Neurological and Neuromuscular Disease*, the *Journal of Neurology*, and *Amiotrophic Lateral Sclerosis and Frontotemporal Degeneration*. He is supported by KAKENHI grants from MEXT/JSPS, Japan (21229011); grants from the Ministry of Welfare, Health and Labor of Japan; and CREST from the JST. Go to Neurology.org for full disclosures.

Received October 10, 2013. Accepted in final form February 19, 2014.

REFERENCES

1. Kennedy WR, Alter M, Sung JH. Progressive proximal spinal and bulbar muscular atrophy of late onset: a sex-linked recessive trait. *Neurology* 1968;18:671–680.
2. La Spada AR, Wilson EM, Lubahn DB, Harding AE, Fischbeck KH. Androgen receptor gene mutations in X-linked spinal and bulbar muscular atrophy. *Nature* 1991;352:77–79.
3. Sobue G, Hashizume Y, Mukai E, Hirayama M, Mitsuma T, Takahashi A. X-linked recessive bulbospinal neuropathy: a clinicopathological study. *Brain* 1989;112:209–232.
4. Katsuno M, Tanaka F, Adachi H, et al. Pathogenesis and therapy of spinal and bulbar muscular atrophy (SBMA). *Prog Neurobiol* 2012;99:246–256.
5. Katsuno M, Adachi H, Kume A, et al. Testosterone reduction prevents phenotypic expression in a transgenic mouse model of spinal and bulbar muscular atrophy. *Neuron* 2002;35:843–854.
6. DeJager S, Bry-Gauillard H, Bruckert E, et al. A comprehensive endocrine description of Kennedy's disease revealing androgen insensitivity linked to CAG repeat length. *J Clin Endocrinol Metab* 2002;87:3893–3901.
7. Li M, Nakagomi Y, Kobayashi Y, et al. Nonneural nuclear inclusions of androgen receptor protein in spinal and bulbar muscular atrophy. *Am J Pathol* 1998;153:695–701.
8. Adachi H, Katsuno M, Minamiyama M, et al. Widespread nuclear and cytoplasmic accumulation of mutant androgen receptor in SBMA patients. *Brain* 2005;128:659–670.
9. Yu Z, Dadgar N, Albertelli M, et al. Androgen-dependent pathology demonstrates myopathic contribution to the Kennedy disease phenotype in a mouse knock-in model. *J Clin Invest* 2006;116:2663–2672.
10. Soraru G, D'Ascenzo C, Polo A, et al. Spinal and bulbar muscular atrophy: skeletal muscle pathology in male patients and heterozygous females. *J Neurol Sci* 2008;264:100–105.
11. Querin G, D'Ascenzo C, Peterle E, et al. Pilot trial of clenbuterol in spinal and bulbar muscular atrophy. *Neurology* 2013;80:2095–2098.
12. Gdynia HJ, Kurt A, Endruhn S, Ludolph AC, Sperfeld AD. Cardiomyopathy in motor neuron diseases. *J Neurol Neurosurg Psychiatry* 2006;77:671–673.
13. Wilde AA, Antzelevitch C, Borggrefe M, et al. Proposed diagnostic criteria for the Brugada syndrome: consensus report. *Circulation* 2002;106:2514–2519.
14. Antzelevitch C, Brugada P, Borggrefe M, et al. Brugada syndrome: report of the second consensus conference: endorsed by the Heart Rhythm Society and the European Heart Rhythm Association. *Circulation* 2005;111:659–670.
15. Hashizume A, Katsuno M, Banno H, et al. Longitudinal changes of outcome measures in spinal and bulbar muscular atrophy. *Brain* 2012;135:2838–2848.
16. Banno H, Katsuno M, Suzuki K, et al. Phase 2 trial of leuprorelin in patients with spinal and bulbar muscular atrophy. *Ann Neurol* 2009;65:140–150.
17. Katsuno M, Adachi H, Minamiyama M, et al. Disrupted transforming growth factor-beta signaling in spinal and bulbar muscular atrophy. *J Neurosci* 2010;30:5702–5712.
18. Tanaka F, Sobue G, Doyu M, et al. Differential pattern in tissue-specific somatic mosaicism of expanded CAG trinucleotide repeats in dentatorubral-pallidolusian atrophy, Machado-Joseph disease, and X-linked recessive spinal

- and bulbar muscular atrophy. *J Neurol Sci* 1996;135:43–50.
19. Makiyama T, Akao M, Tsuji K, et al. High risk for bradyarrhythmic complications in patients with Brugada syndrome caused by SCN5A gene mutations. *J Am Coll Cardiol* 2005;46:2100–2106.
 20. Fukuyama M, Ohno S, Wang Q, et al. L-type calcium channel mutations in Japanese patients with inherited arrhythmias. *Circ J* 2013;77:1799–1806.
 21. Atsuta N, Watanabe H, Ito M, et al. Natural history of spinal and bulbar muscular atrophy (SBMA): a study of 223 Japanese patients. *Brain* 2006;129:1446–1455.
 22. Fernandez-Rhodes LE, Kokkinis AD, White MJ, et al. Efficacy and safety of dutasteride in patients with spinal and bulbar muscular atrophy: a randomised placebo-controlled trial. *Lancet Neurol* 2011;10:140–147.
 23. Morimoto S, Uemura A, Hishida H. An autopsy case of Brugada syndrome with significant lesions in the sinus node. *J Cardiovasc Electrophysiol* 2005;16:345–347.
 24. Asai H, Hirano M, Udaka F, et al. Sympathetic disturbances increase risk of sudden cardiac arrest in sporadic ALS. *J Neurol Sci* 2007;254:78–83.
 25. Mizusawa Y, Wilde AA. Brugada syndrome. *Circ Arrhythm Electrophysiol* 2012;5:606–616.
 26. Veerakul G, Nademanee K. Brugada syndrome: two decades of progress. *Circ J* 2012;76:2713–2722.
 27. Matsuo K, Akahoshi M, Nakashima E, et al. The prevalence, incidence and prognostic value of the Brugada-type electrocardiogram: a population-based study of four decades. *J Am Coll Cardiol* 2001;38:765–770.
 28. Sakabe M, Fujiki A, Tani M, Nishida K, Mizumaki K, Inoue H. Proportion and prognosis of healthy people with coved or saddle-back type ST segment elevation in the right precordial leads during 10 years follow-up. *Eur Heart J* 2003;24:1488–1493.
 29. Schmidt BJ, Greenberg CR, Allingham-Hawkins DJ, Spriggs EL. Expression of X-linked bulbospinal muscular atrophy (Kennedy disease) in two homozygous women. *Neurology* 2002;59:770–772.
 30. Katsuno M, Adachi H, Doyu M, et al. Leuprorelin rescues polyglutamine-dependent phenotypes in a transgenic mouse model of spinal and bulbar muscular atrophy. *Nat Med* 2003;9:768–773.
 31. Chevalier-Larsen ES, O'Brien CJ, Wang H, et al. Castration restores function and neurofilament alterations of aged symptomatic males in a transgenic mouse model of spinal and bulbar muscular atrophy. *J Neurosci* 2004;24:4778–4786.
 32. Nedelsky NB, Pennuto M, Smith RB, et al. Native functions of the androgen receptor are essential to pathogenesis in a *Drosophila* model of spinobulbar muscular atrophy. *Neuron* 2010;67:936–952.
 33. Shimizu W, Matsuo K, Kokubo Y, et al. Sex hormone and gender difference: role of testosterone on male predominance in Brugada syndrome. *J Cardiovasc Electrophysiol* 2007;18:415–421.
 34. Querin G, Melacini P, D'Ascenzo C, et al. No evidence of cardiomyopathy in spinal and bulbar muscular atrophy. *Acta Neurol Scand* 2013;128:e30–e32.
 35. Gallagher MM, Forleo GB, Behr ER, et al. Prevalence and significance of Brugada-type ECG in 12,012 apparently healthy European subjects. *Int J Cardiol* 2008;130:44–48.
 36. Bezzina CR, Barc J, Mizusawa Y, et al. Common variants at SCN5A-SCN10A and HEY2 are associated with Brugada syndrome, a rare disease with high risk of sudden cardiac death. *Nat Genet* 2013;45:1044–1049.
 37. Calloe K, Refaat MM, Grubb S, et al. Characterization and mechanisms of action of novel NaV1.5 channel mutations associated with Brugada syndrome. *Circ Arrhythm Electrophysiol* 2013;6:177–184.
 38. Mo K, Razak Z, Rao P, et al. Microarray analysis of gene expression by skeletal muscle of three mouse models of Kennedy disease/spinal bulbar muscular atrophy. *PLoS One* 2010;5:e12922.
 39. Minamiyama M, Katsuno M, Adachi H, et al. Naratriptan mitigates CGRP1-associated motor neuron degeneration caused by an expanded polyglutamine repeat tract. *Nat Med* 2012;18:1531–1538.
 40. Mok NS, Tong CK, Yuen HC. Concomitant-acquired long QT and Brugada syndromes associated with indapamide-induced hypokalemia and hyponatremia. *Pacing Clin Electrophysiol* 2008;31:772–775.

The Premier Event for *the* Latest Research on Concussion

Registration is now open for The Sports Concussion Conference—*the* premier event on sports concussion from the American Academy of Neurology—set for July 11 through 13, 2014, at the Sheraton Chicago Hotel & Towers in Chicago. You won't want to miss this one-of-a-kind opportunity to learn the very latest scientific advances in diagnosing and treating sports concussion, post-concussion syndrome, chronic neurocognitive impairment, and controversies around gender issues and second impact syndrome from the world's leading experts on sports concussion. Early registration ends June 9, 2014. Register today at AAN.com/view/ConcussionConference.

Antiandrogen Flutamide Protects Male Mice From Androgen-Dependent Toxicity in Three Models of Spinal Bulbar Muscular Atrophy

Kayla J. Renier, Sandra M. Troxell-Smith, Jamie A. Johansen, Masahisa Katsuno, Hiroaki Adachi, Gen Sobue, Jason P. Chua, Hong Sun Kim, Andrew P. Lieberman, S. Marc Breedlove, and Cynthia L. Jordan

Neuroscience Program (K.J.R., S.M.T.-S., S.M.B., C.L.J.), Michigan State University, E Lansing, Michigan 48824–1101; College of Medicine (J.A.J.), Central Michigan University, Mt Pleasant Michigan 48859; Department of Neurology (M.K., H.A., G.S.), Nagoya University Graduate School of Medicine, Nagoya, Japan 466–8550; and Department of Pathology (J.P.C., H.S.K., A.P.L.), University of Michigan, Ann Arbor, Michigan 48109

Spinal and bulbar muscular atrophy (SBMA) is a late-onset, progressive neurodegenerative disease linked to a polyglutamine (polyQ) expansion in the androgen receptor (AR). Men affected by SBMA show marked muscle weakness and atrophy, typically emerging midlife. Given the androgen-dependent nature of this disease, one might expect AR antagonists to have therapeutic value for treating SBMA. However, current work from animal models suggests otherwise, raising questions about whether polyQ-expanded AR exerts androgen-dependent toxicity through mechanisms distinct from normal AR function. In this study, we asked whether the nonsteroidal AR antagonist flutamide, delivered via a time-release pellet, could reverse or prevent androgen-dependent AR toxicity in three different mouse models of SBMA: the AR97Q transgenic (Tg) model, a knock-in (KI) model, and a myogenic Tg model. We find that flutamide protects mice from androgen-dependent AR toxicity in all three SBMA models, preventing or reversing motor dysfunction in the Tg models and significantly extending the life span in KI males. Given that flutamide effectively protects against androgen-dependent disease in three different mouse models of SBMA, our data are proof of principle that AR antagonists have therapeutic potential for treating SBMA in humans and support the notion that toxicity caused by polyQ-expanded AR uses at least some of the same mechanisms as normal AR before diverging to produce disease and muscle atrophy. (*Endocrinology* 155: 2624–2634, 2014)

Spinal and bulbar muscular atrophy (SBMA) is an X-linked recessive disease marked by progressive muscle weakness and atrophy. This disease is linked to a CAG repeat expansion (>40) in the first exon of the androgen receptor (AR) gene located on the X chromosome (1). Recent work in several animal models of SBMA suggests that this neurodegenerative disease depends on male levels of androgens (2–6), potentially explaining the strict male bias of this disease. Evidence also supports the androgen dependence of SBMA in humans (7, 8). Thus, AR antagonists such as flutamide, which are traditionally used to

treat androgen-dependent prostate cancer, may offer therapeutic benefits for men with SBMA. However, current data from animal models suggest flutamide either drives AR toxicity or fails to prevent it (9–11)

In this study, we ask whether continuous exposure via a time-release pellet can reduce disease symptoms in male mice of three different models of SBMA: the AR97Q transgenic (Tg) model, a knock-in (KI) model, and the myogenic Tg model. Mice in all three mouse models recapitulate the human disease, with only males expressing an androgen-dependent loss of motor function (3, 4, 6, 7, 12, 13).

ISSN Print 0013-7227 ISSN Online 1945-7170
Printed in U.S.A.

Copyright © 2014 by the Endocrine Society
Received August 12, 2013. Accepted April 10, 2014.
First Published Online April 17, 2014

Abbreviations: AR, androgen receptor; KI, knock-in; polyQ, polyglutamine; SBMA, spinal and bulbar muscular atrophy; Tg, transgenic; Wt, wild type.

AR97Q Tg males globally express a full-length human AR allele encoding 97 glutamines in the N-terminal domain of the AR protein (4), whereas KI males express a humanized AR protein harboring a 113-polyglutamine tract in the N-terminal domain (3). Finally, Tg males in the myogenic model overexpress a wild-type (Wt) rat AR allele exclusively in skeletal muscle fibers (6). Castration spares or rescues androgen-dependent loss-of-motor function in the two Tg models and prevents androgen-dependent early death in the KI model. We tested flutamide in these three genetically distinct SBMA mouse models, reasoning that if flutamide was efficacious in three different models, such results would be compelling evidence that flutamide may have therapeutic value for human SBMA. Currently there are no effective treatments for SBMA. We find that flutamide protects against androgen-dependent AR toxicity in all three models. These results, along with recent reports showing beneficial effects of another AR antagonist in a cell model of SBMA (14), suggest that AR antagonists, either alone or in combination with agents that reduce T production, may be an effective treatment strategy for men with SBMA.

Materials and Methods

Mice in the AR97Q and the myogenic models were maintained on a C57BL/6 background and mice in the KI model were maintained on a 129S1/SVLMJ background. All mice were weaned 21 days after birth, genotyped using previously described PCR (3, 4, 6), and group housed with food and water provided ad libitum. Animal procedures were approved by the Michigan State University Institutional Animal Care and Use Committee and in compliance with the National Institutes of Health's guidelines for the care and use of experimental animals.

Time-release flutamide pellets (Innovative Research of America; 100 mg flutamide/pellet, 21 d release, 5 mg dose/d) were given to juvenile (28 d old) or adult (≥ 90 d old) males. At the start of flutamide treatment, juvenile AR97Q and adult KI males were asymptomatic, whereas adult myogenic males were already significantly impaired. Thus, we asked whether flutamide could prevent the expression of disease for AR97Q and KI males and could reverse disease for myogenic males. Such pellets are designed to continuously release flutamide over a 3-week treatment period. We estimate that such pellets result in serum levels of approximately 30 $\mu\text{g}/\text{mL}$ of flutamide (15). In our initial pilot experiments we used blank pellets supplied by the same company and found that the effects of flutamide were not attributable to nonspecific effects of the pellet per se. However, we also found that the integrity of blank pellets was not maintained in situ, unlike the flutamide pellets, making it difficult to replace them every 3 weeks, as required for the flutamide pellets. For this reason, sham surgery alone served as our control; control animals were exposed to the same surgical procedures as flutamide-treated animals but did not receive a blank pellet. A battery of motor tests was used to assess disease progression as previously

described (3, 5, 6, 16) including the hang test, grip strength test, motor activity in an open field, and rotarod. Body weight was also monitored throughout. At the end of flutamide treatment, blood and tissue were harvested as indicated below (5, 17)

AR97Q model

Four-week-old asymptomatic AR97Q Tg males and age-matched Wt controls were anesthetized using isoflurane and received either flutamide pellets or nothing ($n = 6-8$ mice/group). Flutamide pellets were implanted sc on the back, near the hip, and replaced every 21 days. Animals also received ketoprofen (5 mg/kg sc) before recovering from anesthesia. Sham controls were subjected to the same surgical procedures as mice who received flutamide pellets. Baseline motor function was established on the day of, but prior to, surgery at 4 weeks of age (designated as treatment d 0) and continued on treatment days 3 and 7 and weekly thereafter until 63 days (13 wk of age).

Assessing the effect of flutamide on circulating T levels of gonadally intact males

Flutamide time-release pellets were implanted in 60-day-old gonadally intact Wt male mice ($n = 12$), and blood was collected transcardially a week later to assess the effect of flutamide on serum T levels in Wt males. We also determined the effect of 4 weeks of flutamide exposure in gonadally intact AR97Q Tg males starting at 28 days of age, spanning the time when exposure to androgens triggers motor dysfunction (4). Flutamide pellets were replaced with new pellets after 3 weeks in AR97Q Tg males with control Tg mice subjected to the same procedures but not given flutamide pellets.

Assessing the effects of flutamide on disease progression in castrated AR97Q Tg males

At 4 weeks of age, presymptomatic AR97Q Tg males and age-matched Wt controls were castrated under isoflurane anesthesia and given sc Silastic implants (Dow Corning Inc) containing crystalline T (1.57 mm inner diameter and 3.18 mm outer diameter; 6 mm effective release length). Such implants are designed to release a constant amount of T over time (18) and result in comparable levels of T as found in adult male mice (5). Half of the AR97Q Tg males and Wt controls also received a 100 mg time-release flutamide pellet sc ($n = 11$ mice/group). Care was taken to place T implants and flutamide pellets in separate sc pockets dorsolaterally to ensure maximal contact of each with the surrounding tissue. Ketoprofen (5 mg/kg sc) was also given before recovery. To maintain optimal release, flutamide pellets and/or T implants were replaced every 21 days until AR97Q T-treated Tg controls (no flutamide) showed end-stage disease symptoms (namely, inability to perform the hang test, difficulty righting, obvious decreases in cage activity, and/or matted, un-groomed fur), at which point mice were killed for tissue harvesting. Because control Tg males reached end-stage at markedly different ages (42–84 d), mice were killed in cohorts of four, age matched across the four conditions. Thus, for each T-treated diseased AR97Q male killed, an age-matched experimental Tg male (T + flutamide) and age-matched Wt controls (T + flutamide, or T without flutamide) were killed as a cohort, all having received the same length treatment. Motor function and body weight was evaluated prior to treatment on day 0, and on days

3 and 7, and weekly thereafter until diseased AR97Q males (T but no flutamide) showed end-stage symptoms.

Assessing the effects of flutamide on soluble and aggregated AR based on Western blots and filter trap assays

A separate group of AR97Q Tg and Wt animals at 28 days of age were castrated and implanted with T capsules, with half in each group also receiving flutamide as described above ($n = 4$ per group). When control Tg males reached end stage (described above), they and their corresponding flutamide-treated, age-matched Tg and Wt controls were deeply anesthetized with isoflurane and the left gastrocnemius muscle and lumbar spinal cord were harvested, flash frozen in liquid nitrogen, and stored at -80°C until tissue analysis was performed. Blood was collected transcardially for measuring circulating T titers.

For Western blot analysis, muscle and cord tissue was minced and homogenized on ice in radioimmunoprecipitation assay buffer containing phosphatase and proteinase inhibitors. Lysates were centrifuged at 4°C for 15 minutes at $15000 \times g$ and protein concentration was determined by protein assay (Bio-Rad Laboratories). Protein samples containing $70 \mu\text{g}$ of protein were mixed with $6 \times$ sodium dodecyl sulfate sample buffer and boiled for 5 minutes at 100°C , followed by electrophoresis through 7% sodium dodecyl sulfate-polyacrylamide gels and transfer to nitrocellulose membranes using a semidry transfer apparatus. After blocking in 5% nonfat milk for 1 hour, membranes were incubated in primary antibodies against AR (1:5000, sc-816; Santa Cruz Biotechnology), heat shock protein 90 (1:5000, sc-7947; Santa Cruz Biotechnology), and glyceraldehyde-3-phosphate dehydrogenase (1:40 000, ab8245; Abcam). Immunoreactive proteins were detected by chemiluminescence. For filter trap analysis, lysates were diluted in radioimmunoprecipitation assay buffer to $40 \mu\text{g}$ per sample and vacuumed through a slot-blot apparatus (Hybri-Slot Manifold; Bethesda Research Laboratories) onto $0.22\text{-}\mu\text{m}$ -pore cellulose acetate membranes pre-rinsed in 20% methanol and PBS. Membranes were then washed in PBS and probed for AR as described for Western blots. Densitometry was used to estimate the amount of monomeric (soluble) and aggregate AR in immunoblots and normalized to protein loading controls heat shock protein 90 in spinal cord and glyceraldehyde-3-phosphate dehydrogenase in muscle. Estimates of AR (based on immunoblots and filter trap assays) were also normalized relative to Wt controls (no flutamide).

Knock-in model

Beginning at 90 days of age, asymptomatic gonadally intact KI males and age-matched Wt control males received either time-release flutamide pellets or sham surgery ($n = 9\text{--}10$ mice/group) as described above. No T treatment was given because gonads were not removed from KI males. Flutamide pellets were replaced every 21 days until mice became moribund or died (or up to 300 d of age). Motor function was assessed prior to flutamide treatment at 90 days of age (designated as treatment d 0) and then assessed on treatment days 2, 4, 6, 8, and 14 and weekly thereafter. Rotarod testing was not conducted.

Myogenic model

To prevent perinatal death of the myogenic Tg males, flutamide was administered prenatally via daily sc injections (5 mg

flutamide in $100 \mu\text{L}$ of propylene glycol) to the dams from gestational day 15 to birth on day 21. Although prenatal flutamide rescues Tg males from perinatal death, it does not prevent the later emergence of androgen-dependent disease (6, 19). Adult (122–139 d) gonadally intact Tg males and their age-matched Wt male controls were anesthetized and received flutamide pellets or sham surgery (17–19 animals per group), as described above for AR97Q mice, with treatment for this model lasting 38–42 days. Baseline motor behavior and body weight was collected 2 days prior to surgery, on day 0 (just before surgery), days 1 and 3 of treatment, and then weekly thereafter up to 6 weeks (until d 42). Rotarod testing was not conducted for males in the myogenic model.

Statistical methods

Results were analyzed using SPSS Statistics software. Control (no flutamide) AR97Q Tg males developed end-stage symptoms at markedly different times, resulting in different numbers at different time points during the treatment period, precluding the use of a repeated-measures ANOVA. Hence, we ran independent t tests to probe for significant differences between flutamide-treated and control-treated AR97Q Tg males. Tests were run only at select time points to limit the chances of a type I error. Groups were selected only if they had nonoverlapping standard error bars. Nonetheless, we used a Bonferroni correction, the most stringent correction, to adjust the α -level when more than a single t test was run on the same data set. A two-way ANOVA was used to evaluate the effects of genotype, treatment, and their interaction on the amount of monomeric protein in the Western blots, whereas independent t tests were used to assess significant differences in aggregate AR in Western blots and filter trap assays. Potential effects of flutamide in the myogenic model were assessed using a $2 \times 2 \times 10$ (genotype \times treatment \times day) three-way ANOVA with repeated measures on the third factor. Significant main effects and interactions were followed up with post hoc comparisons using a Bonferroni correction. For some variables, the data did not meet homogeneity of variance assumptions. For these measures, nonparametric statistics were also run to confirm significance found in the ANOVA. Statistical values presented are from the ANOVA but only those also found to be significant using nonparametric tests in those cases in which homogeneity was violated. Values reported in *Results* are means \pm SEM based on the number of animals per group. Significant effects of flutamide on survival in the KI model were determined using the log-rank test.

Results

AR97Q model

Flutamide only transiently prevents disease progression in gonadally intact Tg males

Expression of the SBMA disease phenotype in this model is highly androgen dependent (4). Unlike the potent protective effects of prepubertal castration, flutamide treatment of prepubertal AR97Q males only transiently protected motor function based on the hang test (Figure 1), with significantly longer hang times than control-treated

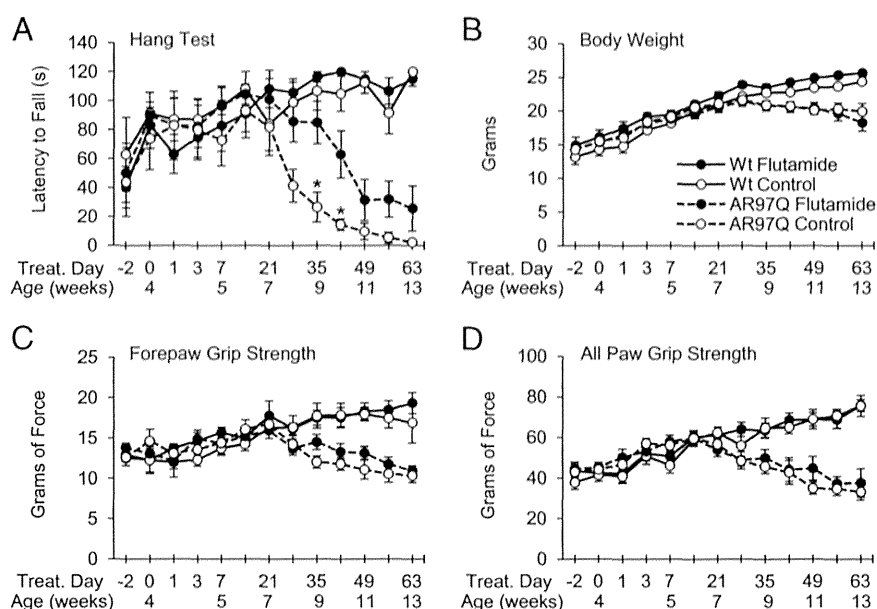


Figure 1. Flutamide only mildly protects gonadally intact AR97Q Tg males from disease. Time-release flutamide pellets given to Tg and Wt males at 28 days of age (treatment d 0) had a significant, albeit transient, sparing effect on muscle strength based on the hang test (A), which slowed the decline in hang test performance. However, flutamide had no sparing effect in gonadally intact AR97Q Tg males on body weight (B) or grip strength (C and D), nor did flutamide affect any measure for Wt males. Plotted data represent the mean \pm SEM of $n = 8$ for flutamide-treated groups and $n = 6$ for control-treated (no flutamide) groups (except $n = 5$ Wt and Tg controls/group at d 56 and 63). *, $P < .017$ based on the Bonferroni correction for comparing flutamide-treated Tg to control-treated Tg based on Student's t tests.

Tgs at 28, 35, and 42 days of treatment ($P = .019$, $P = .005$, $P = .014$, respectively; Figure 1A). However, once the Bonferroni correction was applied (α set at .017), significance of this effect at 28 days dropped below the threshold. Moreover, by 49 days of treatment, flutamide exerted no beneficial effect on motor function. Surprisingly, flutamide had no significant effect on any other measure, including body weight (Figure 1B), grip strength (Figure 1, C and D), number of rears in the open field, stride length, and rotarod performance (data not shown).

Flutamide increases circulating T levels in gonadally intact males

Given the rather mild beneficial effects of flutamide on motor function in AR97Q males during puberty, we exam-

ined the possibility that flutamide might drive circulating T levels up. As predicted (20–22), 1 week of flutamide exposure led to a significant 5-fold increase in the circulating T levels in adult gonadally intact Wt male mice (Table 1, $P = .002$). Of greater significance, 4 weeks of flutamide treatment, starting at postnatal day 28, also induced a significant 3-fold increase in circulating T levels in AR97Q Tg males (Table 1, $P = .021$).

Flutamide fully protects motor function in AR97Q males when T levels are controlled

Although the effect of flutamide on circulating T levels offers one possible explanation for why it might not have protected motor function in AR97Q Tg males, another possibility is that mutant AR disrupts motor function by a novel pathway that is inaccessible to flutamide (11). To directly test this possibility, we averted

the confounding effects of flutamide on circulating T levels by testing flutamide in juvenile AR97Q Tg males that were castrated and given T. The T treatment alone triggered a progressive loss in motor function characteristic of gonadally intact Tg males, whereas flutamide treatment of such castrated T-treated males fully protected their motor function. Although flutamide had only subtle protective effects on body weight (Figure 2A), flutamide maintained the motor function of Tg males at Wt levels. Specifically, flutamide prevented the sharp decline in hang times exhibited by Tg mice that received only T (Figure 2B), resulting in significantly longer hang times at 28 days of flutamide than control-treated Tg mice ($P = .001$, Bonferroni adjusted $\alpha = .017$). Flutamide treatment also fully

Table 1. Flutamide Increases Circulating Levels of T in Gonadally Intact Wt and AR97Q Tg Males

Treatment	Flutamide	Control
One week of treatment in adult Wt males		
Mean \pm SEM, nmol/L	9.33 \pm 3.38 ^a	1.85 \pm 0.50
Range of T values	1.2–39.0	0.4–7.0
Group, n	12	12
Four weeks of treatment (starting P28) in gonadally intact AR97Q males		
Mean \pm SEM, nmol/L	33.38 \pm 7.63 ^a	11.54 \pm 4.76
Range of T values	7.0–57.1	0.6–21.0
Group, n	9	11

The increase in circulating serum levels of T in gonadally intact animals given flutamide may interfere with any beneficial effect of the antiandrogen in these Tg mice. Values are means \pm SEM.

^a $P < .05$ based on a t test.

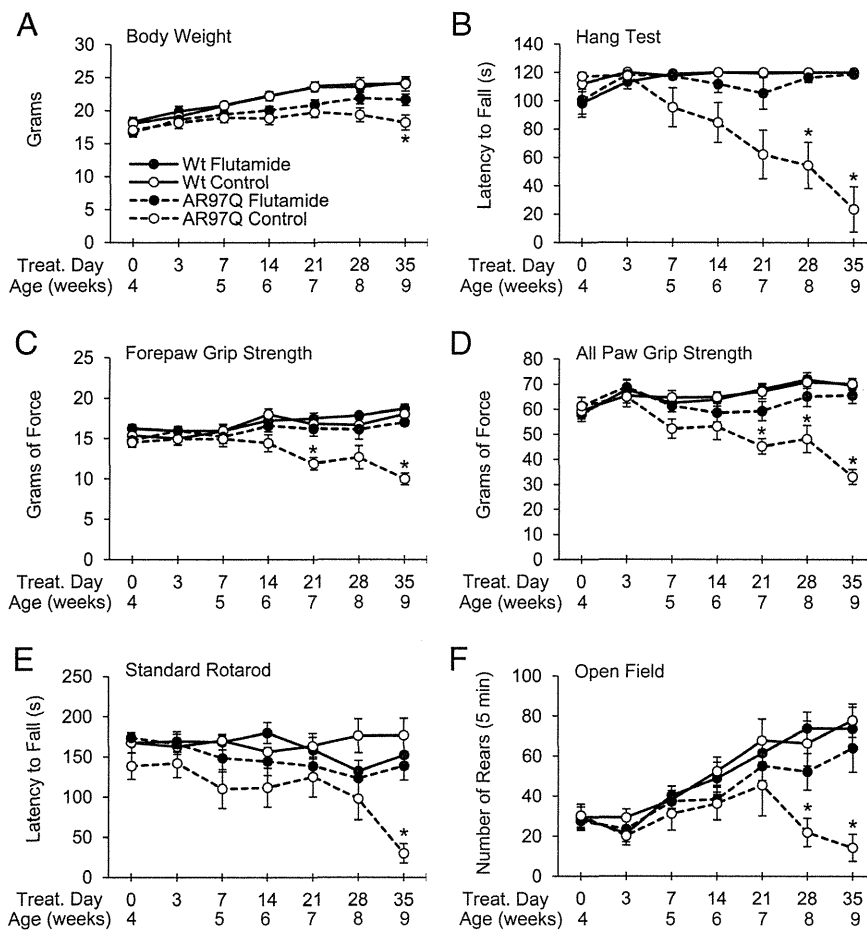


Figure 2. Flutamide fully protects motor function in castrated AR97Q Tg males given T to induce disease. Although flutamide treatment starting at 28 days of age exerts only a partial sparing on body weight (A), it appears to completely spare motor function based on the hang test (B), forepaw and all paw grip strength (C and D), rotarod performance (E), and rearing behavior (assessed for 5 min in an open field; F). *, $P < .05$: flutamide-treated Tg males vs control-treated (no flutamide) Tg males based on Student's *t* tests. Plotted data represents the mean \pm SEM of $n = 11$ per group, with numbers declining to eight per group, control-treated Tg males declining to seven, over time due to disease-related morbidity of control-treated Tgs and corresponding age-matched use of the flutamide-treated Tg males and Wt males for tissue collection. Note that all groups were castrated and received T.

protected grip strength in AR97Q Tg males (Figure 2, C and D), with force measures equivalent to Wt controls and significantly higher starting at 21 days of treatment than Tg mice not exposed to flutamide ($P = .001$ and $P = .0015$ for forepaw and all paws, respectively; Bonferroni adjusted $\alpha = .017$) with the one exception of forepaw grip at 28 days. Flutamide also fully maintained rotarod performance in AR97Q Tg males (Figure 2E), preventing the

drop in performance exhibited by Tg controls at 35 days. Flutamide also prevented the marked decline in rearing behavior (Figure 2F), resulting in significantly more rears in flutamide-treated than control Tg mice at both 28 and 35 days of treatment ($P = .0115$ and $P = .0025$, respectively; corrected $\alpha = .025$). Other measures of motor activity in the open field (eg, total time spent moving) showed a similar sparing effect of flutamide (data not shown). Flutamide also apparently extended life span in this model because only control Tg males reached a moribund state, whereas those given flutamide remained healthy and active, with normal motor function. Importantly, circulating T levels did not differ between flutamide-treated and control-treated Tg mice (Table 2), although they were somewhat higher in the Tg males compared with the Wt males, likely due to differences in body size. We have consistently found that the same size T implant results in higher T levels in smaller animals (23, 24). Regardless, flutamide potently protected the motor function of AR97Q males from the androgen-dependent toxic action of a polyglutamine (polyQ)-expanded AR.

Flutamide affects soluble and aggregated AR in the AR97Q model

We asked whether flutamide treatment affected the amount of monomeric or aggregated AR in T-treated castrated males because decreases in either might underlie the protective effect of flutamide in SBMA pathogenesis. We found that flutamide significantly reduces monomeric AR in the lumbar spinal cord of both Wt and Tg males (Figure 3A and C, $P = .002$ compared with respective Wt and Tg controls). In the gastrocnemius muscle,

Table 2. Flutamide Does Not Increase Circulating Levels of T in T-treated Wt and AR97Q Tg Males When They Are Castrated

AR97Q Castrated, T Treated, \pm Flutamide				
Treatment	Wt Flutamide	Wt Control	AR97Q Flutamide	AR97Q Control
Mean \pm SEM, nmol/L	8.95 \pm 2.423	6.2 \pm 1.114	16.73 \pm 9.423	18.95 \pm 7.793
Range of T values	2.5–27.5	2–12.5	1.5–109.5	2–93.5
Group, n	10	10	11	10

Values are means \pm SEM.

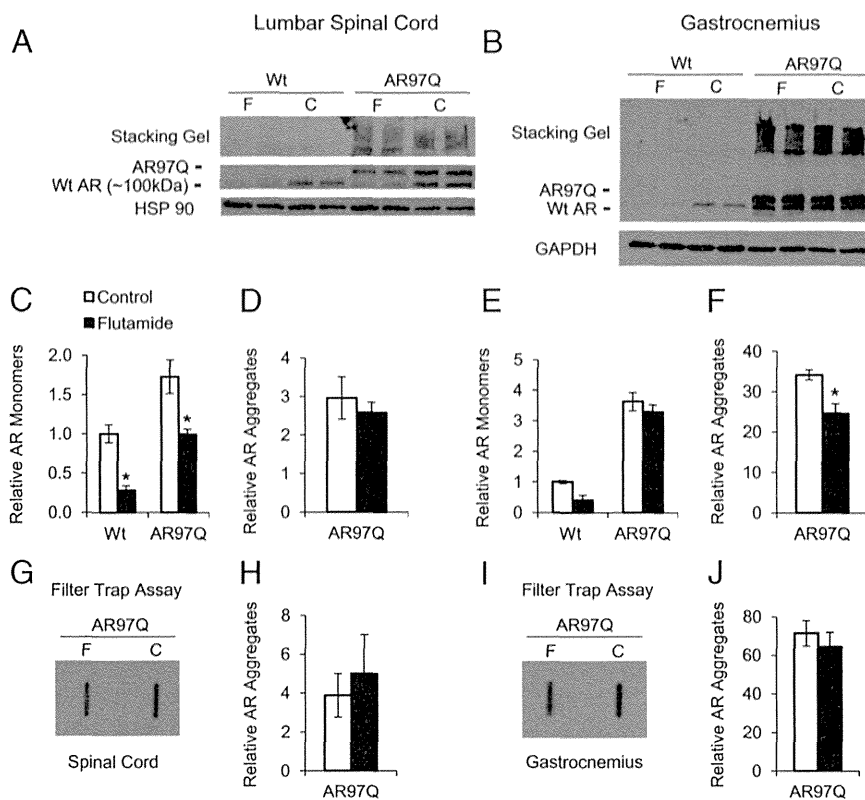


Figure 3. Protection of motor function by flutamide in AR97Q Tg males is associated with reduced monomeric and aggregate AR. Western blots show the effect of flutamide (F) on monomeric and aggregate (in stacking gel) Wt and 97Q AR in the lumbar spinal cord (panel A) and gastrocnemius muscle (panel B) of castrated Wt and Tg mice treated with T compared with T-treated castrates that did not receive flutamide (panel C). Quantitative analysis of monomeric AR shows that flutamide treatment reduces 97Q-AR but only in the spinal cord (C) and not in the muscle (panel E). As expected, flutamide also reduced Wt AR (lower band) but also only in the spinal cord. Also, Western blots show aggregate AR in the stacking gel of both spinal cord (panel A) and gastrocnemius muscle (panel B) of Tg males only. Quantitative analysis of aggregate AR in the stack indicates that flutamide reduces aggregate AR in muscle (panel F) but not in spinal cord (panel D). Note, however, that the spinal cord contains very little aggregate AR compared with muscle, thus limiting our ability to detect differences. Filter-trap assays confirm that aggregated AR is much more abundant in the gastrocnemius muscle (panel J) than lumbar spinal cord (panel H) of AR97Q Tg males and indicates that flutamide has no effect on the amount of AR aggregates in either tissue. Plotted data represent the mean \pm SEM of $n = 4$ mice per group and is normalized relative to control-treated Wt values. *, $P < .05$ based on Student's t tests for aggregate data (panels D, F, H, and J) and by 2 ANOVAs for monomeric data (panels C and E).

however, flutamide did not significantly reduce monomeric AR in either Wt males ($P = .060$, compared with control treated Wt mice) or AR97Q Tg males ($P = .271$, compared with control treated Tg mice; Figure 3, B and E).

same age using the same method of T delivery for both experiments. Regardless, flutamide also fully protected the motor function of AR97Q Tg males in this second experiment (data not shown).

Because there was little or no evidence of AR aggregates in Wt tissue, we limited the quantitative assessment of aggregate AR to Tg samples. Assessing the amount of high-molecular-weight AR in the stack of the Western blots indicates that flutamide modestly reduces the amount of aggregated 97QAR in gastrocnemius muscle but not in the spinal cords of same Tg males (Figure 3, D and F; flutamide-treated vs control treated Tg muscle: $P = .011$). However, data based on filter trap assays suggest that flutamide has no effect on the abundance of AR aggregates in the spinal cord (Figure 3, G and H, $P = .641$) or muscle (Figure 3, I and J, $P = .509$).

We also found that flutamide partially prevented a decrease in gastrocnemius weight caused by disease (flutamide treated Tg mice: 0.096 ± 0.016 g vs control treated Tg mice: 0.060 ± 0.003 g; $P = .023$) but had no effect on muscle weight in Wt males (flutamide treated Wt mice: 0.144 ± 0.011 g vs control treated Wt mice: 0.140 ± 0.002 g; $P = .737$). As expected, muscles from control-treated Wt mice weighed twice as much as those from diseased, control-treated Tg males. We found no difference between treatment groups in circulating T levels (Table 3), although levels were consistently higher in this second experiment than in the first. The reason behind this difference is not clear because treatments began at the

Table 3. Effects of Flutamide on Circulating T Levels in T-treated Castrated Wt and Tg Males Used to Assess Soluble and Aggregated AR Based on Western Blots and Filter Trap Assays

AR97Q Castrated, T Treated, \pm Flutamide				
Treatment	Wt Flutamide	Wt Control	AR97Q Flutamide	AR97Q Control
Mean \pm SEM, nmol/L	28.65 \pm 5.83	17.55 \pm 4.40	36.9 \pm 12.186	22.38 \pm 2.243
Range of T values	18–44.2	15–58	9.9–30	16–25.8
Group, n	4	4	4	4

Values are means \pm SEM.

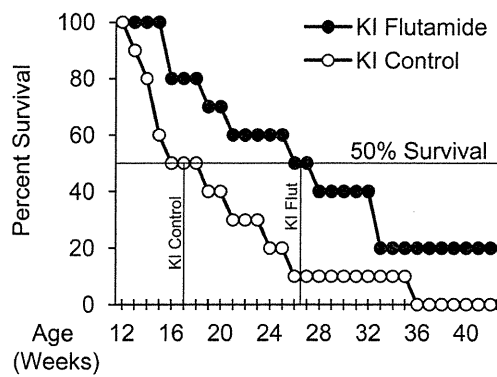


Figure 4. Flutamide treatment beginning at 90 days of age significantly extends the life span of adult KI males. Control-treated KI males reach 50% survival at 17 weeks of age, whereas 50% survival for flutamide-treated KI males is extended to 26.5 weeks, when only 10% of control-treated KIs remain alive. Average life span for flutamide-treated KIs was 199.2 ± 21.7 days compared with 145.4 ± 15.8 days for control-treated KIs (mean \pm SEM) ($n = 10$ KIs per group). A log-rank test indicates a significantly ($P < .05$) improved survival of SBMA KI males conferred by flutamide.

Knock-in model

Flutamide treatment of KI males prolongs life span

Treating 90-day-old gonadally intact KI males with flutamide extended their average life span compared with control-treated KI males (199.2 ± 21.7 vs 145.4 ± 15.8 d, respectively, Figure 4). By 17 weeks of age, 50% of con-

trol-treated KIs had reached end-stage (died or become moribund), compared with only 20% of flutamide-treated KIs. It was a full 2 months later, at 26.5 weeks of age, before 50% of flutamide-treated KIs had reached end-stage. This benefit occurred despite the fact that flutamide increased circulating T levels in gonadally intact KI males (flutamide treated KI males: 14.1 ± 1.62 nmol/L vs flutamide treated, aged matched Wt males: 18.3 ± 4.55 nmol/L vs control treated, age matched Wt males: 7.9 ± 4.01 ; mean \pm SEM). Of note, untreated KI males have circulating T levels comparable with Wt males (25). That flutamide-treated KI males survived significantly longer than control-treated KIs was confirmed based on the log-rank test ($P = .049$). KI males show only mild motor deficits that were, in our hands, not statistically significant (based on hang test, grip strength, or open field; data not shown). KI males also did not show a decline in body weight over the course of disease as is characteristic of AR97Q mice (data not shown). Flutamide also did not affect any of these measures.

Myogenic model

Flutamide treatment improves motor function of chronically impaired Tg males

We also tested the therapeutic potential of flutamide in the myogenic model. We find that flutamide significantly improved motor function of chronically diseased, gonadally intact adult Tg males (122–139 d of age). Note that treatment began when Tg males were fully symptomatic (Figure 5). Based on separate three-way, repeated-measures ANOVA for each measure (hang times, grip strength, etc), significant main effects and interactions between genotype, treatment, and time were found, warranting further post hoc analyses. Separate two-way, repeated-measures ANOVAs were then run to determine whether flutamide significantly affected our measures within each genotype over days. Indeed, we found a significant main effect of flutamide on hang times ($P = .001$) and grip strength (all values of $P = .001$) of Tg males but no effects on these measures in Wt mice. We also found that the effects of flutamide interacted significantly with days of treatment on all measures (all values of $P = .001$) in Tg males, warranting pair-

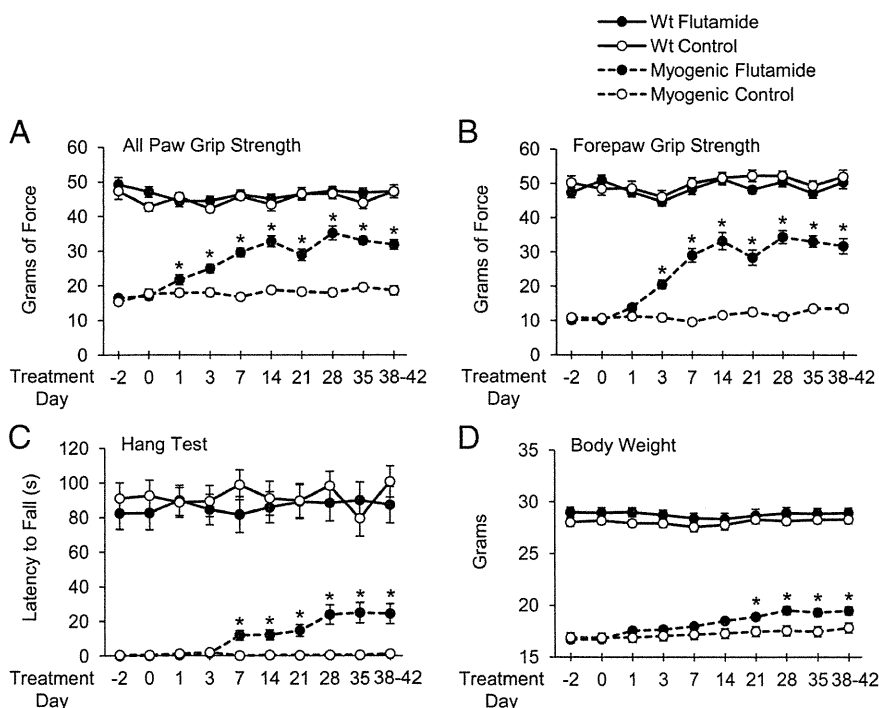


Figure 5. Flutamide significantly improves the motor function of chronically diseased myogenic Tg males that overexpress Wt rat AR only in skeletal muscle fibers. The partial rescue of grip strength (A and B), hang times (C), and body weight (D) for diseased Tg males may reflect increased circulating T caused by flutamide in gonadally intact males, which could interfere with flutamide binding to AR. Plotted data represent the mean \pm SEM for $n = 17$ – 19 animals per group. *, $P < .05$ for flutamide-treated Tgs vs control-treated Tgs based on a three-way ANOVA followed by pairwise comparisons.

wise comparisons between flutamide-treated and control-treated Tg mice. Remarkably, flutamide significantly improved all-paw grip strength within 24 hours (Figure 5A, $P = .004$) with significant improvement in fore-paw grip strength emerging by 72 hours (Figure 5B, $P = .001$). The beneficial effect of flutamide on hang times in Tg males emerged a few days later at 1 week of treatment with significant increases in hang times (Figure 5C, $P = .015$). Finally, flutamide significantly increased the body weight of symptomatic Tg males starting at 14 days (Figure 5D, $P = .035$). Although flutamide clearly mitigated the effects of disease in the myogenic Tg males, their motor function was not fully restored to normal.

Discussion

We examined the therapeutic potential of the AR antagonist flutamide in three genetically distinct male mouse models of SBMA: 1) the AR97Q Tg model broadly expresses a full-length human AR with 97Qs, 2) the KI model expresses a targeted CAG expanded human allele in the first exon of the endogenous AR gene, and 3) the myogenic Tg model expresses Wt rat AR only in skeletal muscle fibers. Despite these genetic differences, each model exhibits male-biased motor dysfunction that is androgen dependent (3, 4, 6). Given the apparent androgen dependence of this disease, AR antagonists were expected to be therapeutic. However, previous reports indicate that the AR antagonist flutamide is neurotoxic in a fly model of SBMA (9, 10), whereas being neither beneficial nor harmful in the AR97Q mouse model (11). Contrary to these findings, we now report that flutamide prevents androgen-dependent motor dysfunction in AR97Q males and reverses androgen-dependent motor dysfunction in myogenic males. Flutamide also greatly ameliorates androgen-dependent early death in KI males. Given that flutamide effectively protects against androgen-dependent AR toxicity in three different mouse models of SBMA, akin to its well-established antagonist action on normal AR function (26–28), our data are proof of principle that flutamide has therapeutic potential for treating SBMA in humans.

Our results are not without caveats. Although clearly showing that flutamide can antagonize the toxic action of an androgen-activated polyQ-AR, flutamide also stimulates an increase in circulating androgens in gonadally intact male mice, limiting the effectiveness of flutamide as a treatment for disease (Figure 1 and Table 1). However, flutamide can potently protect the motor function of castrated AR97Q Tg males that are treated with T to induce the disease (Figure 2). These results demonstrate that flu-

tamide can in fact block the toxic action of a polyQ-expanded AR. Although flutamide also combated androgen-dependent AR toxicity for both KI and myogenic males (Figures 4 and 5), flutamide's efficacy in these models was less complete, likely because KI and myogenic males were gonadally intact. Thus, the use of flutamide to treat SBMA in humans may require adjuvant treatment with other antiandrogens, such as leuprorelin, which limit T production.

Results of a phase two clinical trial for leuprorelin, although promising, indicate only modest beneficial effects overall on motor function (8), which could potentially be enhanced by adjuvant treatment with flutamide. Flutamide combined with leuprorelin is a standard treatment regimen for advanced prostate cancer (29) and has been given to a patient with both SBMA and prostate cancer. Although it was reported that the patient tolerated the treatment well for the 4 years observed, the status of his SBMA symptoms were not reported.

There is some dispute over whether the myogenic model is a legitimate mouse model for SBMA because motor dysfunction in this model is triggered by Wt AR rather than polyQ-expanded AR (1). Although this question is not readily answered, there are several compelling reasons to think that the myogenic model has clinical relevance to SBMA. First and foremost, the disease phenotype displayed by myogenic mice aligns well with that described for SBMA in humans and other mouse models of this disease (2–4, 6). Core features of the disease phenotype include a distinct male bias and androgen-dependent motor dysfunction, both of which myogenic mice show (6). Second, there is growing precedence linking both mutant and Wt alleles of the same gene to the same neurodegenerative disease. Notable recent examples include superoxide dismutase 1 linked to amyotrophic lateral sclerosis (30) and α -synuclein linked to Parkinson's disease (31). Wt AR has also been shown to exert comparable androgen-dependent toxicity as the polyQ-expanded AR in both mouse and fly models of SBMA and likely triggers toxicity through common molecular pathways (32, 33). Finally, up to 17% of affected men diagnosed with SBMA show the expected cluster of symptoms [slowly progressing motor dysfunction coupled with signs of decreased androgen sensitivity (eg, gynecomastia) and elevated serum creatine kinase levels] but nonetheless lack the polyQ expansion in their AR gene (34, 35). Thus, it is possible that dysregulation of AR expression per se causes SBMA in some individuals.

Although KI males show only mild motor deficits, which in this cohort of mice was not detected, we did detect the androgen-dependent early death reported for this model (3). Flutamide significantly ameliorated this